

GEOLOGICAL, GEOPHYSICAL, AND THERMAL CHARACTERISTICS OF THE SALTON SEA GEOTHERMAL FIELD, CALIFORNIA

DELAND W. YOUNKER, PAUL W. KASAMEYER and JOHN D. TEWHEY

Earth Sciences Division, University of California, Lawrence Livermore National Laboratory, Livermore, CA 94550 (U.S.A.)

(Received February 10, 1981; revised and accepted August 27, 1981)

ABSTRACT

Younger, L.W., Kasameyer, P.W. and Tewhey, J.D., 1982. Geological, geophysical, and thermal characteristics of the Salton Sea Geothermal Field, California. *J. Volcanol. Geotherm. Res.*, 12: 221–258.

The Salton Sea Geothermal Field is the largest water-dominated geothermal field in the Salton Trough in Southern California. Within the trough, local zones of extension among active right-stepping right-lateral strike-slip faults allow mantle-derived magmas to intrude the sedimentary sequence. The intrusions serve as heat sources to drive hydrothermal systems.

We can characterize the field in detail because we have an extensive geological and geophysical data base. The sediments are relatively undeformed and can be divided into three categories as a function of depth: (1) low-permeability cap rock, (2) upper reservoir rocks consisting of sandstones, siltstones, and shales that were subject to minor alterations, and (3) lower reservoir rocks that were extensively altered. Because of the alteration, intergranular porosity and permeability are reduced with depth. Field permeability is enhanced by renewable fractures, i.e., fractures that can be reactivated by faulting or natural hydraulic fracturing subsequent to being sealed by mineral deposition.

In the central portion of the field, temperature gradients are high near the surface and lower below 700 m. Surface gradients in this elliptically shaped region are fairly constant and define a thermal cap, which does not necessarily correspond to the lithologic cap. At the margin of the field, a narrow transition region, with a low near-surface gradient and an increasing gradient at greater depths, separates the high temperature resource from areas of normal regional gradient. Geophysical and geochemical evidence suggest that vertical convective motion in the reservoir beneath the thermal cap is confined to small units, and small-scale convection is superimposed on large-scale lateral flow of pore fluid.

Interpretation of magnetic, resistivity, and gravity anomalies help to establish the relationship between the inferred heat source, the hydrothermal system, and the observed alteration patterns. A simple hydrothermal model is supported by interpreting the combined geological, geophysical, and thermal data. In the model, heat is transferred from an area of intrusion by lateral spreading of hot water in a reservoir beneath an impermeable cap rock.

INTRODUCTION

The Salton Sea Geothermal Field is one of several water-dominated geo-

thermal fields in the Salton Trough, a sediment-filled rift valley that represents the landward extension of the Gulf of California into North America. The area has been the subject of intensive geologic investigation for several reasons. It is a seismically active region and a significant link in the transition from the divergent plate boundary of the East Pacific Rise to the transform boundary of the San Andreas fault system (Elders et al., 1972; Lomnitz et al., 1970; Elders and Biehler, 1975). Hot brines are present at depth in the field making the area ideally suited for the study of active hydrothermal alteration and ore deposition (Helgeson, 1968; Muffler and White, 1969; Skinner et al., 1967). Finally, from a more applied viewpoint, it is one of the largest and most accessible geothermal resource areas in North America (Towse, 1975; Renner et al., 1975; Nathenson and Muffler, 1975; Biehler and Lee, 1977; Younker and Kasameyer, 1978). With detailed understanding, this region can be exploited efficiently.

Our purpose is to characterize the thermal anomaly and show its relationship to the geological and geophysical features of the field. In the first section we review the geological characteristics of the field. This description is based largely on information from logs of 16 geothermal wells and from drill cuttings and core samples from 3 wells (Tewhey, 1977). The information is broadly consistent with other recent descriptions of the field (McDowell and Elders, 1979). In the second section we briefly review the geophysical characteristics of the field, with emphasis on aspects relating to the nature of the heat source. In the final section we analyze in detail the subsurface temperatures and the surface gradient data to infer the mechanisms of heat transfer throughout the system. We then summarize the information from these three sets of observations and arrive at an overview of the geothermal system. In a future paper we will present a quantitative heat-transfer model consistent with these characteristics and the overall tectonic setting.

THE GEOLOGIC CHARACTERISTICS OF THE SALTON SEA GEOTHERMAL FIELD

Geologic setting

The Salton Trough is the northern portion of a structural and topographic basin extending from southern California to the southern end of the Gulf of California. From its origin in the Miocene (Dibblee, 1954; Hamilton, 1961) until mid-Pleistocene (Downs and Woodward, 1961), the trough received sediments from the Colorado River. In mid-Pleistocene, possibly during a period when the sea level was low, the Colorado River delta was built westward across the trough from Yuma, Arizona. Deltaic sediments accumulated during this time and the northern portion of the basin, i.e., the Salton Trough, was topographically separated from the Gulf of California. The Salton Sea represents the latest in a long sequence of inland seas that have occupied the trough since the Pleistocene (Van de Kamp, 1973).

Geological (Dibblee, 1954) and geophysical evidence (Biehler et al., 1964)

shows that the sequence is approximately 6000 m thick. Fine-grained rocks along the margins of the trough are 4097-m Wilson No. 1 well largely of detritus from the trough on the east and deltaic sediments in the trough consisting predominantly of feldspar, clay minerals,

The present description is based on 16 geothermal wells (Tewhey, 1977). The wells in the west-central portion are Nos. 2 and 3 and Woolsong No. 1, 1064 m deep, respectively. Specific samples were

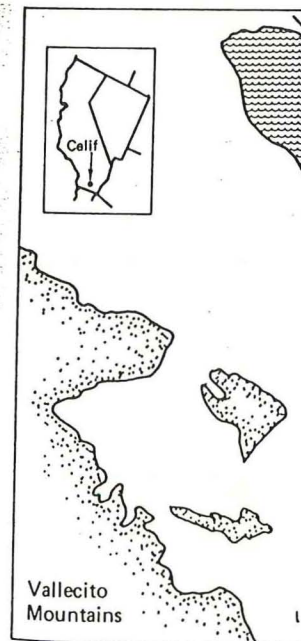


Fig. 1. Location of the Salton Valley (after Elders et al., 1972). The map shows locations of wells in the

filled rift valley that represents
into North America. The
investigation for several reasons.
link in the transition from the
to the transform boundary
(1972; Lomnitz et al., 1970);
at depth in the field making
hydrothermal alteration and ore
(1969; Skinner et al., 1967).

of the largest and most
America (Towse, 1975; Renner
er and Lee, 1977; Younker
ing, this region can be

omally and show its relation-
of the field. In the first section
field. This description is based
al wells and from drill cuttings
The information is broadly
field (McDowell and Elders,
geophysical characteristics
the nature of the heat source.
surface temperatures and the
heat transfer throughout the
these three sets of observa-
system. In a future paper we
consistent with these character-

SALTON SEA GEOTHERMAL FIELD

structural and topographic
southern end of the Gulf of
(1954; Hamilton, 1961)
(1), the trough received sedi-
, possibly during a period
a was built westward
iments accumulated during
, the Salton Trough, was
ia. The Salton Sea
as that have occupied the

nce (Biehler et al., 1964)

shows that the sequence of sedimentary rocks in the Salton Trough is approximately 6000 m thick. Based on results of field work in the folded sedimentary rocks along the margins of the trough and examination of cuttings from the 4097-m Wilson No. 1 well near Brawley, the 6000-m sequence is composed largely of detritus from the Colorado River. Only minor contributions appear to have come from the Chocolate Mountains and Peninsular ranges bordering the trough on the east and west (Muffler and White, 1969). The unaltered deltaic sediments in the Salton Trough have a rather uniform composition consisting predominantly of quartz and calcite and subordinately of dolomite, feldspar, clay minerals, mica, and accessory minerals.

The present description of reservoir geology is based on information in logs from 16 geothermal wells and drill cutting and core samples from 3 wells (Tewhey, 1977). The wells from which samples were obtained are located in the west-central portion of the Salton Sea Geothermal Field, i.e., Magmamax Nos. 2 and 3 and Woolsey No. 1 (Fig. 1). The three wells are 1331, 1219, and 1064 m deep, respectively. The cutting samples were examined microscopically and specific samples were selected for petrographic, X-ray diffraction, and

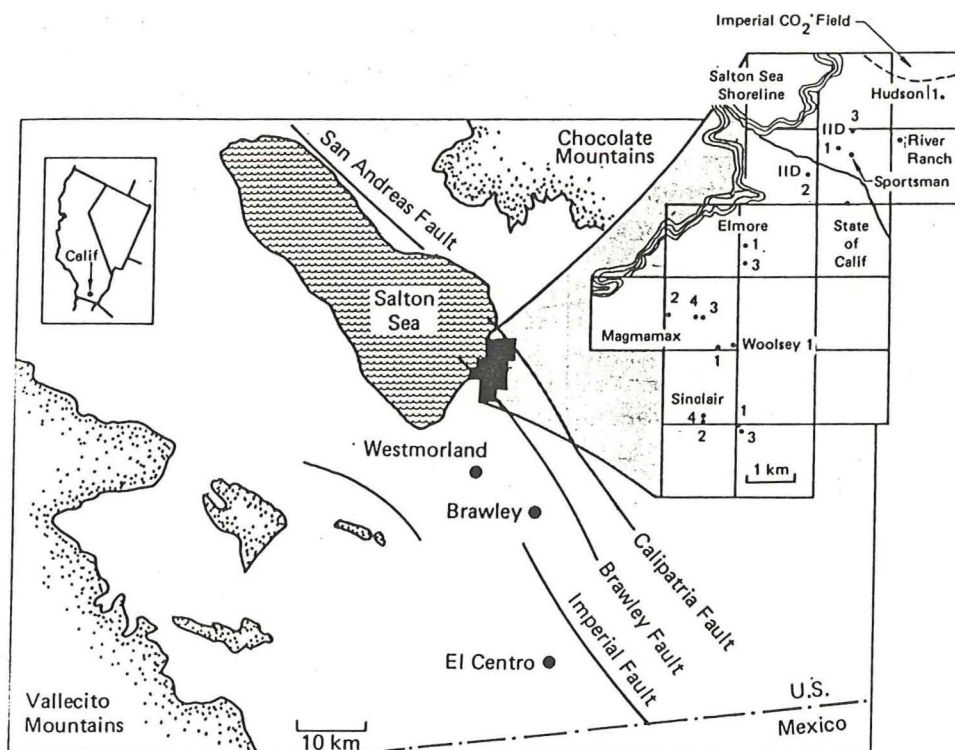


Fig. 1. Location of the Salton Sea Geothermal Field and nearby faults in the Imperial Valley (after Elders et al., 1972). Basement rocks are indicated by stippling. The inset shows locations of wells in the field.

microprobe analyses. The petrographic analyses and porosity measurements were done on core samples. The drill cutting samples yielded evidence of a sedimentary sequence in the study area from the surface to below 1300 m that can be divided into three categories: (1) cap rock, (2) upper, slightly altered, reservoir rocks, and (3) lower, extensively altered, reservoir rocks. This is shown in Fig. 2.

Sedimentary sequence

The cap rock. The cap rock of a geothermal system is the thick layer of low permeability rock that overlies the more permeable reservoir rocks. It can serve both as a barrier for circulating convection currents and as a thermal insulator, thereby contributing to the increase in temperature in the geothermal system.

In the Salton Sea Geothermal Field, the cap rock thickness is variable and, generally, is thickest (~700 m) in the northern portion of the field and thinnest

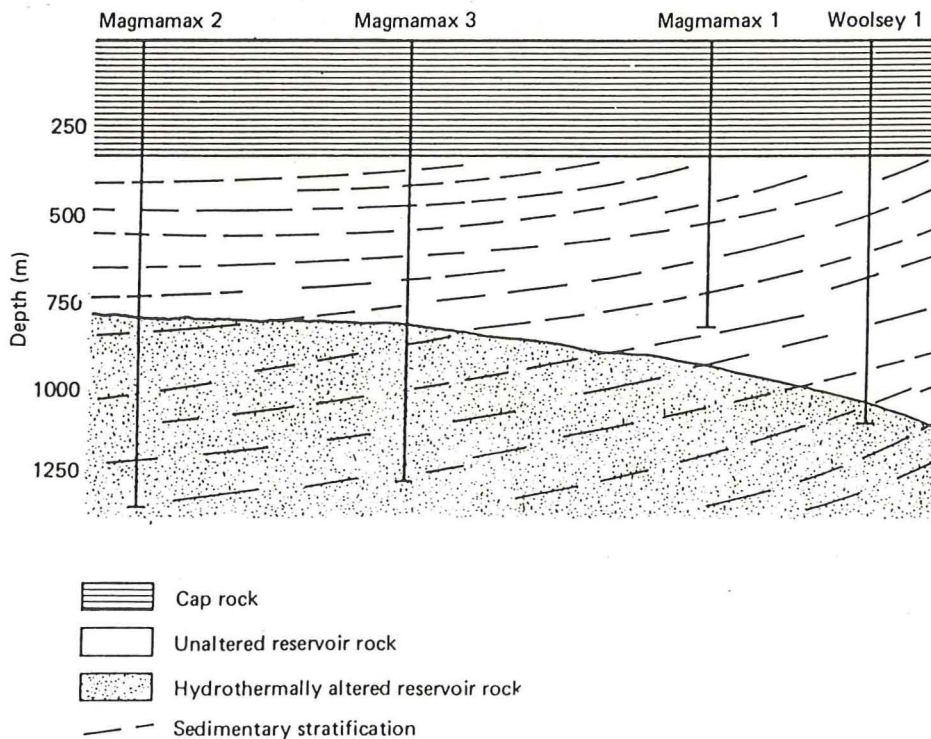


Fig. 2. East-west cross section through the Magmamax and Woolsey wells in the Salton Sea Geothermal Field. The three rock types, i.e., cap rock, slightly altered reservoir rock, and hydrothermally altered reservoir rock, are classifications based on petrographic analysis. Boundaries between rock types are those determined in this report. The orientation of strata in the reservoir rock is shown by dashed lines.

(~250 m) in the south. Physical data from log wells, the cap rock is present in the cap. The clay, silt, sand and gravel rock sequence consist of a carbonate matrix. The interlocking textures of the cap rock reduce its permeability. Gypsum cementation of the cap rock field is limited to environmental diagenesis, gypsum is present in the cap. The relatively thick cap rock is indicative of tectonic compression in the basin since its thickness is variable.

Facca and Tonani (1972) in a hydrothermal system cap rock. Direct evidence of the Salton Trough minute veinlets and fluid inclusions precipitating crack production and occur in reservoir rock. See a later section.

Upper reservoir rock. The cuttings examined for hot brines penetrated the cap rock. The effects of brine-induced alteration are principally silicification. The kaolinite and nectrochlore are characteristic (Muffler and White, 1972).

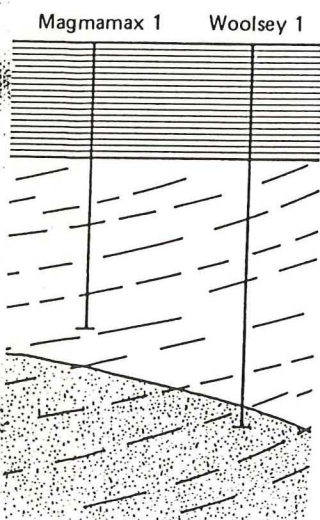
With the exception of the Magmamax well, the cap rock is only by means of careful studies. These second-order petrophysical properties are variable.

The sharp transition between the cap rock (unaltered reservoir rock) deposited in the northern portion of the basin and the hydrothermally altered reservoir rock (extensively altered reservoir rock) deposited in the southern portion of the basin is interpreted as a conformable sequence (Muffler and White, 1972) consider the evidence as a conformable sequence.

and porosity measurements
 logs yielded evidence of a
 surface to below 1300 m that
 (2) upper, slightly altered,
 reservoir rocks. This is

is the thick layer of low
 reservoir rocks. It can
 currents and as a thermal
 temperature in the geothermal

Its thickness is variable and,
 location of the field and thinnest



Woolsey wells in the Salton Sea
 slightly altered reservoir rock, and
 based on petrographic analysis.
 report. The orientation of

(~250 m) in the southern portion (Randall, 1974). Based on analysis of geophysical data from logs and observation of cutting samples near the Magmamax wells, the cap rock is 340 to 370 m thick (Fig. 2). Two distinct layers are present in the cap. The material in the upper 200 m consists of unconsolidated clay, silt, sand and gravel. The material from 200 m to the bottom of the cap rock sequence consists primarily of anhydrite-rich evaporite layers, often in a carbonate matrix. The evaporite layers are consolidated and not friable, and the interlocking textures of anhydrite and carbonate grains indicate low permeability. Gypsum commonly precipitates from sea water. However, its stability field is limited to environments near the surface, because during burial and diagenesis, gypsum is dehydrated and converted to anhydrite (Berner, 1971). The relatively thick sequence of evaporite-rich deposits that make up the cap rock is indicative of the long sequence of intermittent Salton Seas that existed in the basin since its isolation from the Gulf of California.

Facca and Tonani (1967) have shown empirically that hot water circulating in a hydrothermal system can produce alteration and deposition along flow paths in the cap rock and, thereby, reduce permeability. In this manner, a geothermal system can be self-sealing by producing or restoring its own cap rock. Direct evidence of the self-sealing phenomenon was provided by Batzle and Simmons (1976), who examined samples of cap rock from the Dunes area of the Salton Trough using the scanning electron microscope. They interpreted minute veinlets and fluid inclusion trains as microcracks that were healed by minerals precipitating from circulating fluids. There is evidence to suggest that crack production and subsequent sealing are not limited to the cap rock but occur in reservoir rocks at the Salton Sea field as well. This will be discussed in a later section.

Upper reservoir rock. Technically, there are no unaltered sediments in the cuttings examined for this study. Thermal springs at the surface indicate that hot brines penetrated and permeated the entire sedimentary section. The effects of brine-induced alterations in the uppermost reservoir rocks are principally silicification and clay mineral reactions. An example of the latter is that kaolinite and montmorillonite are transformed to chlorite or illite (Muffler and White, 1969).

With the exception of pyrite mineralization, the rock alteration above 800 m in the Magmamax wells and above 1000 m in the Woolsey well is detectable only by means of careful X-ray diffraction analysis or detailed petrographic studies. These secondary alterations did not result in marked changes in the petrophysical properties (e.g., porosity and permeability) of the reservoir rocks.

The sharp transition between reservoir rocks and the overlying cap rock is interpreted as representing the boundary between marine sediments (reservoir rock) deposited in the Gulf of California and lacustrine sediments (cap rock) deposited in the Salton Trough after it was isolated from the southern portion of the basin in the mid-Pleistocene. Dibblee (1954) and Dutcher et al. (1972) consider the entire Miocene/Pleistocene section in the Salton Trough as a conformable sequence.

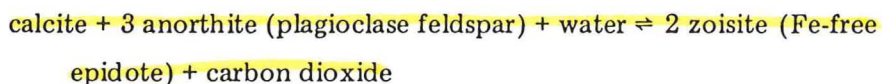
In the Magmamax Nos. 2 and 3 wells, the zone of slightly altered reservoir rocks is approximately 480 m thick, extending from a depth of 340 m to nearly 820 m. In Woolsey No. 1, the zone is 660 m thick, from 340 to 1000 m. The thickness of this zone increases to the east and, to a lesser extent, to the north and is related to the heat distribution in the geothermal field. The slightly altered sequence in the Magmamax and Woolsey wells consists of indurated sandstones, siltstones, shales, and a few thin coal seams. The sandstone contains subangular clastic grains of quartz with minor feldspar, mica, chlorite, and lithic fragments. The rocks exhibit varying degrees of calcite cementation and intergranular porosity ranging from 10 to 30%.

The first appearance of epidote in reservoir rocks is used to mark the transition to high-rank alteration. The epidote producing reaction is temperature dependent and corresponds approximately to the present-day 280°C isotherm.

Hydrothermally altered reservoir rocks. The mineralogical and textural changes in deep-seated rocks in the Salton Sea Geothermal Field can be attributed to hydrothermal alteration in an open system with a large mass-transfer of chemical constituents. The important variables seem to have been permeability, temperature, brine composition, and original rock composition. At the temperatures characteristic of the Magmamax wells ($\leq 300^\circ\text{C}$), sandstones, and siltstones were appreciably altered, but the less permeable shales were relatively little affected. Heat-induced metamorphism occurs in shales in the deeper portions of the reservoir.

The hydrothermally altered deltaic sediments that constitute the reservoir rocks can be described chemically by the complex system $\text{K}_2\text{O}-\text{Na}_2\text{O}-\text{CaO}-\text{MgO}-\text{FeO}-\text{Fe}_2\text{O}_3-\text{Al}_2\text{O}_3-\text{SiO}_2-\text{CO}_2-\text{H}_2\text{O}-\text{S}$. To interpret the observed mineral assemblages, as well as those that might be encountered at depth, it is necessary to reduce the complex system to the simple well-studied subsystem of $\text{CaO}-\text{Al}_2\text{O}_3-\text{SiO}_2-\text{CO}_2-\text{H}_2\text{O}$. The isobaric phase relations at 2 kbar in the subsystem as a function of temperature and mole fraction CO_2 are depicted in Fig. 3.

Calcite is a principal component of upper, slightly altered, reservoir rocks and epidote is common in the lower rocks. The gradual disappearance of calcite with depth coincides with the development of epidote as an alteration product. The mineralogical observations and the presence of abundant CO_2 at shallow depths in the geothermal field can be accounted for by the evolution of CO_2 through the reaction:



The slope of the univariant line representing this reaction (Fig. 3) is near infinity, thus, the sign of dT/dX_{CO_2} is difficult to determine experimentally. If dT/dX_{CO_2} is positive, the transition from calcite to zoisite (epidote) will occur as the temperature increases. If the sign of dT/dX_{CO_2} is negative, the

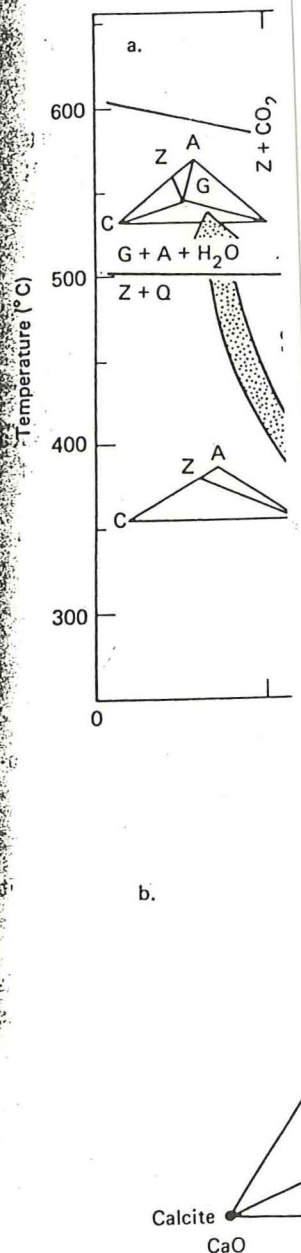


Fig. 3. (a) Temperature versus $\text{SiO}_2-\text{CO}_2-\text{H}_2\text{O}$ system modified with a possible reaction path, with petrologic observations phase relations. (b) Detail of

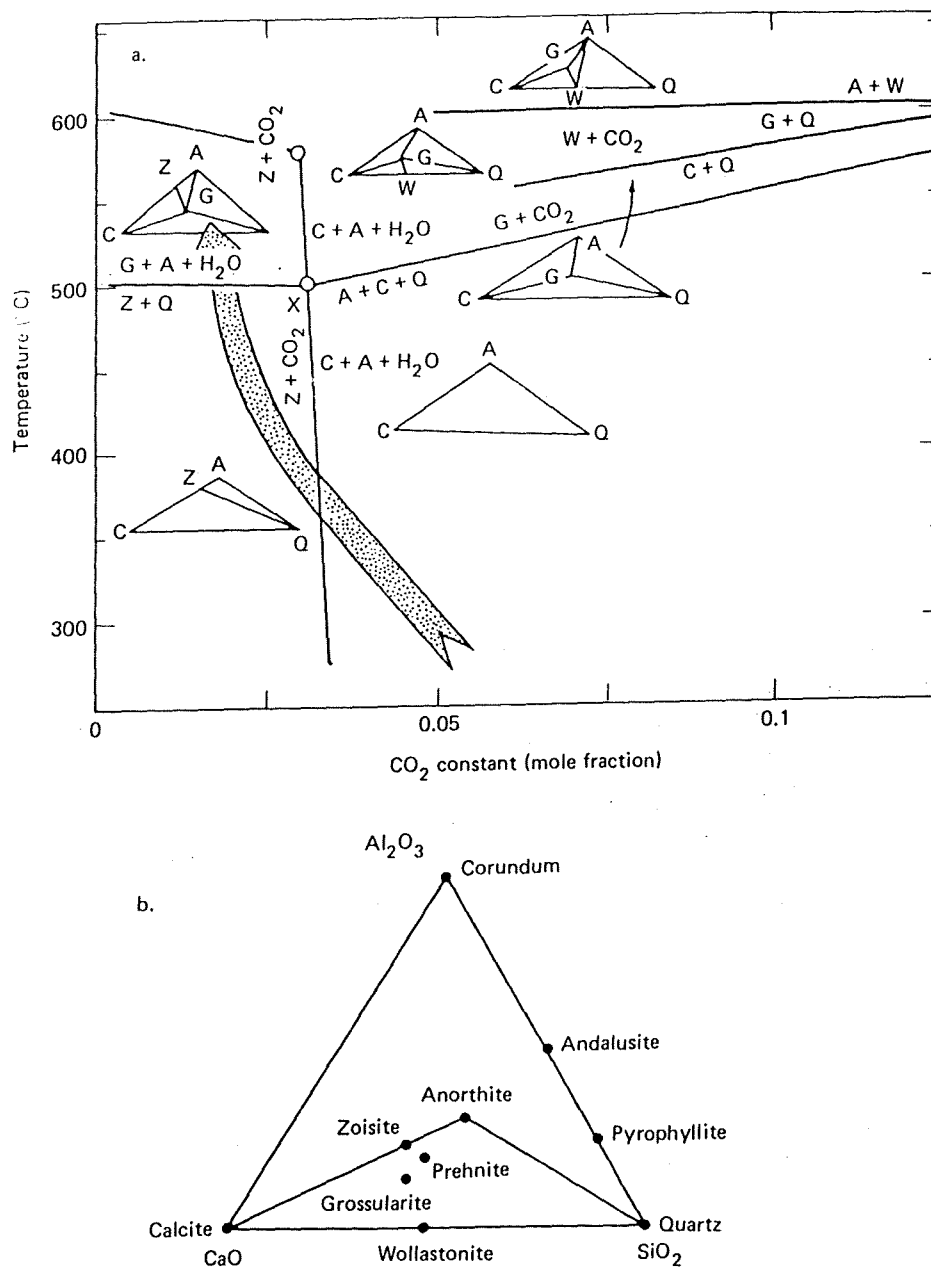


Fig. 3. (a) Temperature versus CO_2 content plotted at $P_{\text{fluid}} = 2$ kbar for the $\text{CaO-Al}_2\text{O}_3\text{-SiO}_2\text{-CO}_2\text{-H}_2\text{O}$ system modified from Storre and Nitsch (1972). The shaded arrow represents a possible reaction path, with depth, for the Salton Sea Geothermal Field that is consistent with petrologic observations. The calcite-anorthite-quartz (CAQ) triangle is used to depict phase relations. (b) Detail of CAQ triangle.

of slightly altered reservoir
 from a depth of 340 m to
 1000 m thick, from 340 to 1000 m
 d, to a lesser extent, to the
 geothermal field. The slight-
 ly wells consists of indurated
 seams. The sandstone contains
 spar, mica, chlorite, and
 of calcite cementation and

is used to mark the transi-
 g reaction is temperature
 present-day 280°C isotherm.

ological and textural changes
 Field can be attributed to
 large mass-transfer of chem-
 have been permeability,
 composition. At the temper-
 0°C), sandstones, and silt-
 able shales were relatively
 in shales in the deeper

at constitute the reservoir
 system $\text{K}_2\text{O-Na}_2\text{O-CaO-}$
 et the observed mineral
 er at depth, it is neces-
 ell-studied subsystem of
 ions at 2 kbar in the sub-
 sion CO_2 are depicted in

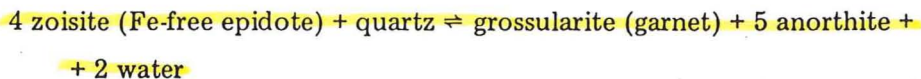
y altered, reservoir rocks
 dual disappearance of calcite
 ote as an alteration product.
 abundant CO_2 at shallow
 by the evolution of CO_2

2 zoisite (Fe-free

ction (Fig. 3) is near in-
 mine experimentally.
 zoisite (epidote) will
 dX_{CO_2} is negative, the

calcite to zoisite transition will be largely pressure dependent. Therefore, if the sign of dT/dX_{CO_2} is either positive or negative, a mechanism exists for the transition of epidote to calcite as the depth increases.

Grossularite-andradite garnet has been found in cuttings from the deepest wells in the Salton Sea field (Kendall, 1976; McDowell and McCurry, 1977); therefore, the reaction path shown in Fig. 3 can be extended into the garnet field by the reaction:



The nature of the transition from slightly altered to more extensively altered rocks in the Salton Sea field was determined by petrographic, X-ray diffraction, and electron microprobe analyses. Both the chemical (mineralogical) and physical changes that result from alteration were studied. Epidote is first seen at 811 m in Magmamax 2, at 826 m in Magmamax 3 and at 1006 m in Woolsey 1. Muffler and White (1969) report first seeing epidote at 1052 m in IID No. 1 well and 1167 m in Sportsman No. 1 well. Although the data base is scanty, the contours of the epidote isograd, i.e., the first appearance of epidote, are concentric with the heat axis as defined by Randall (1974) and the pattern of subsurface isotherms as determined by Palmer (1975).

High-rank hydrothermal alteration of the reservoir rocks in the Salton Sea Geothermal Field has reduced porosity and permeability. Epidote and silica are the principal pore filling minerals produced during high temperature alteration. They replace calcite and anhydrite, the cementing agents produced during diagenesis. The process of the self-sealing geothermal field (Facca and Tonani, 1967), discussed earlier, is beneficial when it creates an impermeable cap rock over a shallow geothermal reservoir, but it can be detrimental when it reduces porosity and permeability in reservoir rocks.

Porosity was determined on core samples from geothermal wells at the Salton Sea (see Fig. 4), and a reduction of porosity was noted with depth. This is common in sedimentary basins and is enhanced in the Salton Sea Geothermal Field by hydrothermal alteration.

In the area studied, data from geophysical logs and drill cores indicate that the reservoir strata dip westward toward the center of the geothermal resource at approximately 10 degrees. In the presence of the vertical porosity gradient, the dipping strata become less porous and less permeable from the periphery of the field toward the center of the heat axis (Fig. 2).

Significance of fracture porosity and permeability

Fractures provide a substantial portion of the permeability and reservoir capacity in a number of geothermal fields, e.g., Geysers, Otake, Larderello, Wairakai, and Broadlands (Facca, 1973). The primary intergranular porosity in a reservoir is subject to irreversible self-sealing; however, fractures can be

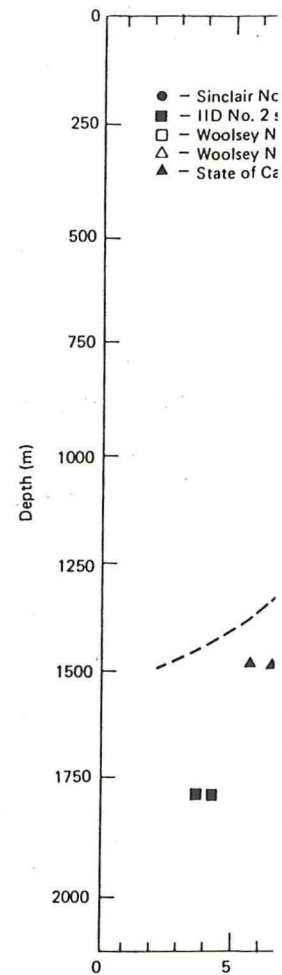


Fig. 4. Measured porosity Salton Sea Geothermal Field.

considered to have reactivated after the system may be either fault areas with active tensional fractures from high fluid pressure.

The hydrothermal reservoirs in the Salton Sea Geothermal Field are extensively fractured from a few micrometers to meters. Active spreading zone fractures in the reservoir

dependent. Therefore, if a mechanism exists for reuses.

cuttings from the deepest well and McCurry, 1977); extended into the garnet

garnet) + 5 anorthite +

l to more extensively d by petrographic, X-ray a the chemical (mineralogical) re studied. Epidote is first max 3 and at 1006 m in being epidote at 1052 m in l. Although the data base the first appearance of d by Randall (1974) and y Palmer (1975).

ir rocks in the Salton Sea bility. Epidote and silica ng high temperature altera- ing agents produced dur- rmal field (Facca and it creates an impermeable can be detrimental when it

othermal wells at the was noted with depth. This the Salton Sea Geothermal

d drill cores indicate that of the geothermal resource vertical porosity gradient, able from the periphery ()).

neability and reservoir ers, Otake, Larderello, y intergranular porosity vever, fractures can be

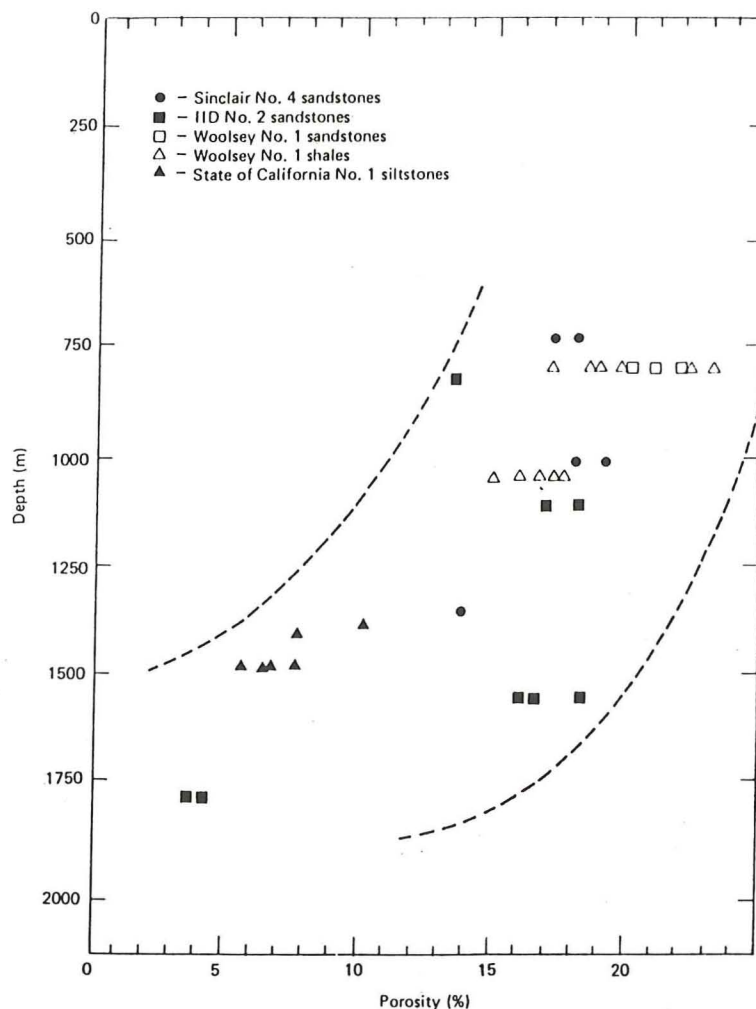


Fig. 4. Measured porosity versus depth for cores from five geothermal wells in the Salton Sea Geothermal Field.

considered to have renewable porosity, or permeability, or both, because they can be reactivated after being filled or sealed. The fracture producing mechanism may be either faulting (many major geothermal fields are located in areas with active tensional tectonics) or natural hydraulic fracturing resulting from high fluid pressures in the reservoir (Grindley and Browne, 1976).

The hydrothermally altered reservoir rocks in the Salton Sea Geothermal Field are extensively fractured, especially the shales. Fracture widths range from a few micrometers to 1 mm. The location of the Salton Sea Field on an active spreading zone (Elders et al., 1972) ostensibly can account for the many fractures in the reservoir.

Evidence for the renewability of fracture porosity and permeability after sealing is found in the form of (1) calcite-filled veins in which the calcite was mechanically twinned and deformed after deposition, indicating there was renewed stress on an old fracture; (2) calcite-filled veins reactivated (refractured) and then refilled with epidote; and (3) anhydrite veins that reveal two or more episodes of fracturing and deposition when viewed with cathodoluminescence (see Fig. 5). These observations suggest that the seismic activity in the Salton Trough may maintain fracture permeability in the reservoir.

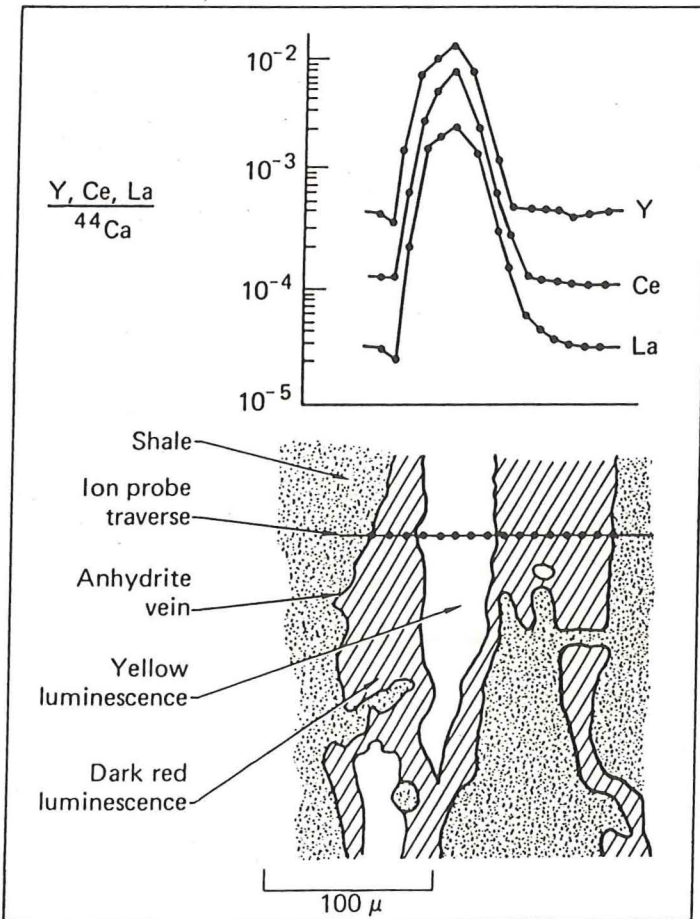


Fig. 5. Calcite and epidote veins in shale from > 900-m depths in the Salton Sea Geothermal Field. Ion-microprobe traverses were made across zoned anhydrite grains to determine the geochemical basis for differences in luminescent intensity. The position of data points in the graph is seen on the ion-microprobe traverse. Positive concentration-anomalies of Y, Ce, and La correspond to zones of yellow luminescence.

Subsurface structure

Subsurface sediment in the Salton Sea field south section extends the Sinclair No. 3 well west section extends passes the Magmama (SP) log, the principal permeable sandstone locate boundaries be

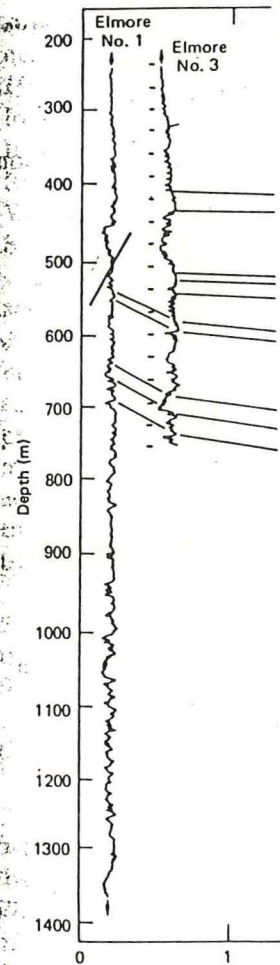


Fig. 6. Spontaneous potential from Elmore No. 1 to Sinclair No. 3.

and permeability after
in which the calcite was
, indicating there was
veins reactivated (refrac-
ite veins that reveal two
viewed with cathodo-
that the seismic activity
ility in the reservoir.

Subsurface structure

Subsurface sedimentary strata were correlated among 10 geothermal wells in the Salton Sea field. Two cross sections were constructed. The north to south section extends for 4 km from the Elmore No. 1 well in the northern to the Sinclair No. 3 well in the southern portion of the field (Fig. 6). An east to west section extends for 2 km in the central portion of the field and encompasses the Magmamax and Woolsey wells (Fig. 2). The spontaneous potential (SP) log, the principal tool used for correlation purposes, is useful to detect permeable sandstones, determine qualitative indications of bed shaliness, and locate boundaries between sand and shale units.

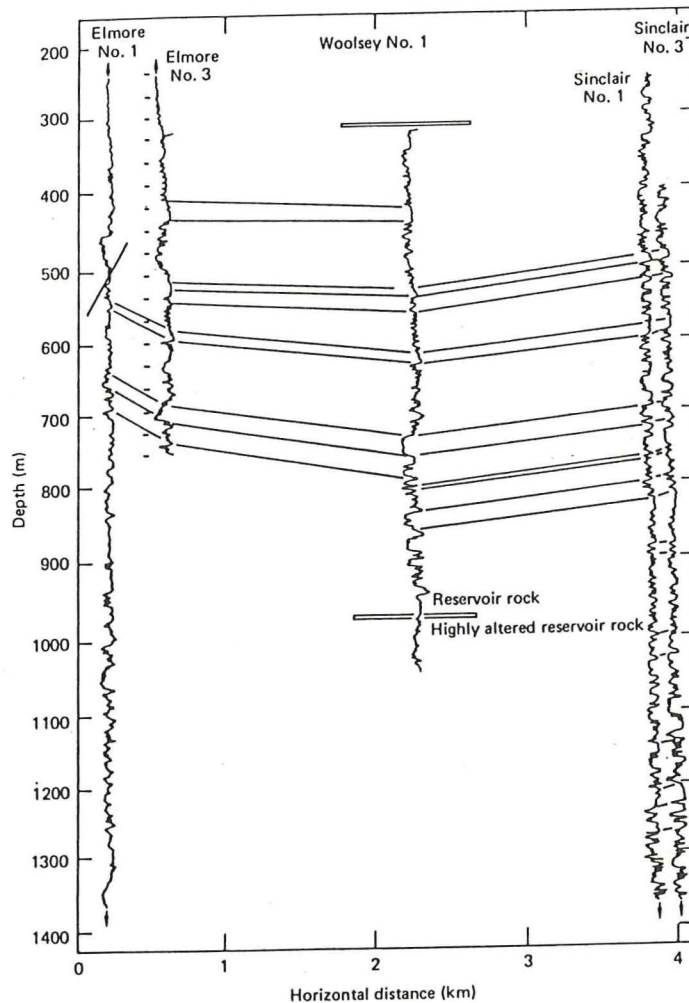


Fig. 6. Spontaneous potential (SP) log correlations of five wells extending north to south from Elmore No. 1 to Sinclair No. 3 in the Salton Sea Geothermal Field.

the Salton Sea Geothermal
grains to determine the
position of data points in the
anomalies of Y, Ce,

The evaporate and carbonate-rich cap rock sequence (most of which is not seen in Fig. 6) produces a flat, featureless SP curve of little use for detailed correlation. The potential for correlation is also somewhat reduced in the zone of hydrothermally altered reservoir rock. Hydrothermal alteration promotes the growth of new minerals in the pore space of permeable sandstones and in shale partings and fractures. The alteration limits the response of diverse rock types to the SP log that, in turn, makes correlating more difficult.

The structural picture emerging from these and other cross sections is one of a broad syncline with an east to west axis approximately perpendicular to the axis of the Salton Trough. The syncline has a shallow westward plunge toward the center of the trough, and there is a general tendency for north to south thickening of individual sedimentary units.

Igneous activity

The Salton Sea Geothermal Field has five rhyolite buttes arranged along a northeast trend at the southern end of the sea. These buttes are spaced 3–4 km apart, and were extruded over Quaternary alluvium. Robinson et al. (1976) noted that these rhyolites were similar in composition to those on islands of the East Pacific Rise and that basaltic inclusions within the rhyolites from the Salton Sea buttes are similar to the low-potassium tholeiitic basalts from the rise. This bimodal rhyolite plus basalt association is a common feature of regions characterized by tensional tectonics. Evidence suggesting subsurface igneous activity in the region includes the gravity and magnetic anomalies discussed below and the presence of altered basaltic and silicic dikes and sills in several of the geothermal wells at a depth of 1–2 km (Robinson et al., 1976).

GEOPHYSICAL CHARACTERISTICS OF THE SALTON SEA GEOTHERMAL FIELD

Tectonic setting

The Salton Sea Geothermal Field is a significant link in the transition from the divergent plate boundary of the East Pacific Rise to the transform boundary of the San Andreas fault system. North of the Salton Sea, and within the Salton Trough, the right lateral San Andreas fault system consists of three subparallel strands, i.e., the Banning-Mission Creek, the San Jacinto, and the Elsinore. South of the Salton Sea, these strands lose their character and merge into a series of smaller, less distinct, subparallel faults. Based on recent seismicity within the Imperial Valley, the most important faults are the side-stepping Imperial, Brawley, and Calipatria (Fig. 1).

Lomnitz et al. (1970) noted that the spreading centers in the Gulf of California are offset by right-stepping en echelon faults, in a manner similar to that displayed in the Imperial Valley on a smaller scale. They suggested that the tectonic framework in the northern portion of the Gulf of California and

the Salton Trough as transform faults. In the Salton Trough, they postulate anomalies near Cerro Prieto. Expanded and refined data from the trough show gaps between en echelon faults. Fuis et al. (1975) label this in the region is strike-slip of offset strike-slip movement is right-lateral.

The general model is supported by gravity anomalies centered on the trough. Fuis et al. (1971) found a high velocity zone in the Imperial Valley. They formed from the Imperial Valley. Vertical leveling data from the Salton Trough consistent with the model.

Seismicity in the region and swarms of small earthquakes (Johnson, 1979). The motion between the plates and activity has been related to tectonic processes (Hill, 1977). Major events have not been revealed in epicenter locations. The combination of seismicity and the transform model (Wells, 1970).

The Salton Sea Geothermal Field in the Salton Trough, where rifting can be directly related to the Salton Sea helped to

Geophysical anomalies

Gravity, magnetic anomalies in the Salton Sea Geothermal Field. The geothermal area is approximately 100 km². Elders et al. (1972) show that the magnetic anomalies of the sediments result from dikes and sills intruding into the

The magnetic survey of the Salton Sea (Elders, 1936) reveal the presence of

ence (most of which is not of little use for detailed somewhat reduced in the zone thermal alteration promotes permeable sandstones and in response of diverse rock more difficult. other cross sections is one approximately perpendicular to shallow westward plunge a tendency for north to

the buttes arranged along a the buttes are spaced 3–4 km Robinson et al. (1976) on to those on islands of within the rhyolites from m tholeiitic basalts from is a common feature of the suggesting subsurface d magnetic anomalies and silicic dikes and sills km (Robinson et al.,

A GEOTHERMAL FIELD

in the transition from to the transform the Salton Sea, and s fault system consists creek, the San Jacinto, s lose their character l parallel faults. Based on mportant faults are . 1). rs in the Gulf of , in a manner similar to They suggested that Gulf of California and

the Salton Trough could be understood by considering these strike-slip faults as transform faults connected by short spreading centers. Within the Salton Trough, they postulated, active ridge segments account for the geothermal anomalies near Cerro Prieto and the Salton Buttes. Elders et al. (1972) expanded and refined the model using geophysical, petrological, and geodetic data from the trough. They suggested active spreading centers occur in tensional gaps between en echelon strike-slip faults. Elders and Biehler (1975) and Hill et al. (1975) label these areas leaky transform faults; the dominant movement in the region is strike slip, with spreading taking place in a rather diffuse zone of offset strike-slip faults. The complex interaction of extensional and strike-slip movement is responsible for the overall structure of the trough.

The general model of crustal rift formation by leaky transform faulting is supported by gravity, seismic, and leveling data. A gravity maximum in the center of the trough can be explained by 8 km of crustal thinning (Biehler, 1971). Fuis et al. (1982) used over 3000 seismograms from 1300 stations and found a high velocity crust at depths of 10–16 km under two thirds of the Imperial Valley. They interpret this region as having an oceanic-type crust that formed from the intrusion of mantle-derived materials into areas of extension. Vertical leveling data collected since 1900 indicate ongoing deepening of the Salton Trough consistent with the general model of rifting (Lofgren, 1978).

Seismicity in the Salton Trough is characterized by both large earthquakes and swarms of small-magnitude earthquakes (Hill et al., 1975; Sylvester, 1979; Johnson, 1979). The large earthquakes obviously result from the relative motion between the North American and Pacific plates; however, the swarm activity has been related to hydraulic fracturing (Johnson, 1979) or magmatic processes (Hill, 1977). The relationship between the swarm events and the major events has not been established, but the general pattern of seismicity, as revealed in epicenter locations and first motion studies, is consistent with the combination of regional shearing and local extension required by the leaky transform model (Weaver and Hill, 1978).

The Salton Sea Geothermal Field is one of the thermal anomalies within the Salton Trough, where the active processes associated with crustal thinning and rifting can be directly observed. A wide range of geophysical surveys near the Salton Sea helped to detail critical aspects of the hydrothermal system.

Geophysical anomalies associated with the field

Gravity, magnetic and resistivity surveys show many features of the Salton Sea Geothermal Field (Figs. 7–9). A local gravity maximum within the geothermal area is approximately centered on Red Island Rhyolite butte (Fig. 7). Elders et al. (1972) attributed the local anomaly to either an increase in density of the sediments resulting from hydrothermal alteration, or the intrusion of dikes and sills into the sedimentary section, or both.

The magnetic surveys of Griscom and Muffler (1971) and Kelley and Soske (1936) reveal the presence of material with a relatively high susceptibility and

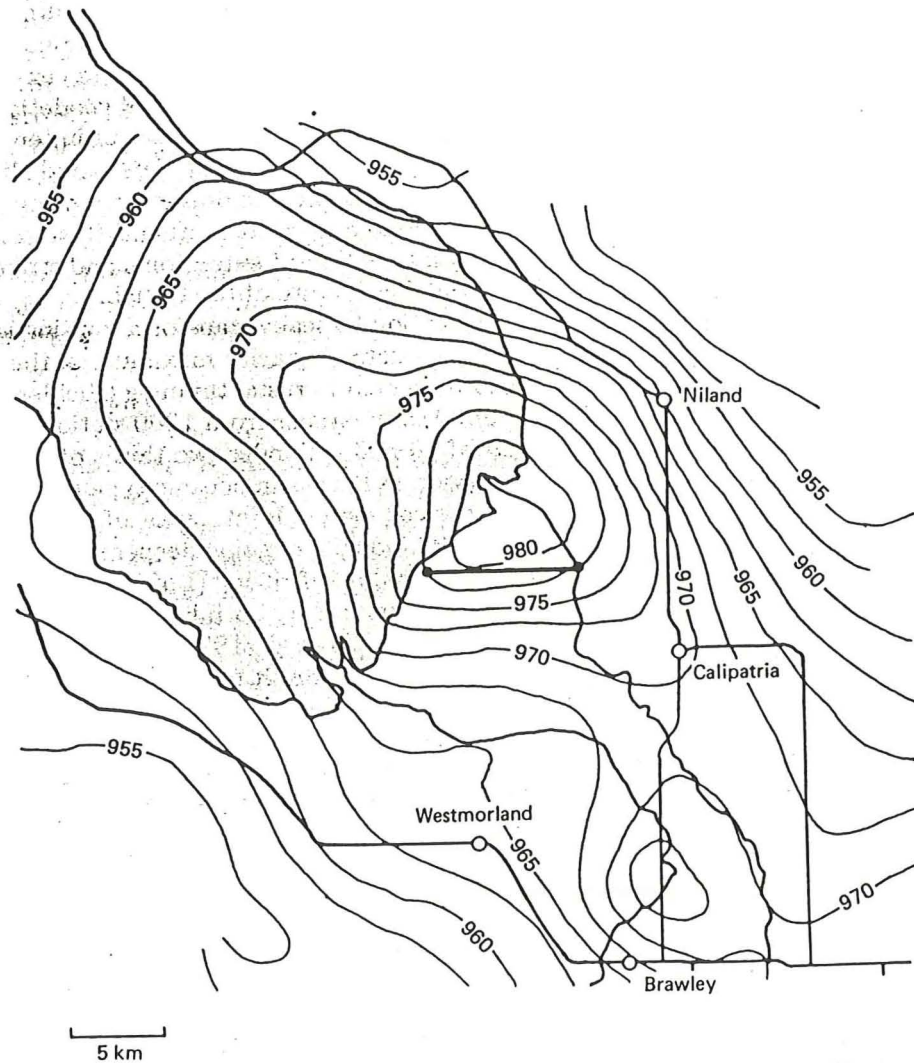


Fig. 7. Bouguer gravity anomaly map of the area near the Salton Sea Geothermal Field (after Biehler, 1971). Heavy solid line shows the position of a seismic refraction profile (refer to Fig. 10). The contour interval is 2.5 mgals.

remanent magnetization near the surface (Fig. 8). Griscom and Muffler separated the major anomaly into three superimposed ones, with the dominant feature a magnetic ridge trending northwest from Calipatria to the middle of the Salton Sea. Two elliptical northeast-trending anomalies are superimposed upon the ridge; and small intense anomalies clearly associated with the volcanic domes are, in turn, superimposed on the elliptical anomalies. They interpreted

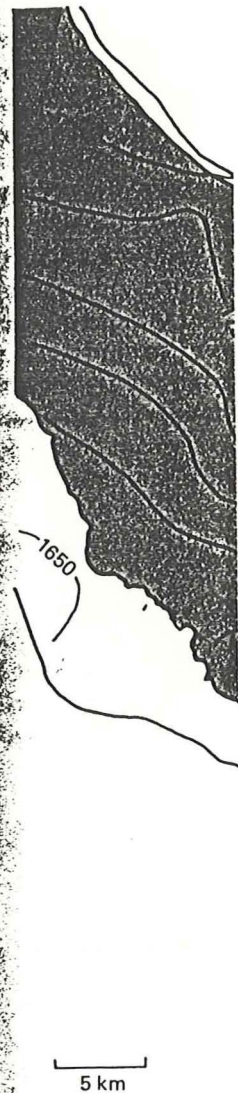


Fig. 8. Aeromagnetic map of the area near the Salton Sea Geothermal Field (after Griscom and Muffler, 1971). The

the magnetic ridge is approximately 1 km wide and the elliptical anomalies are approximately 1 km wide.

Meidav et al. (1971) interpreted the geothermal field. E. The resistivities of less than 10 ohm-meters consisted of 60 south

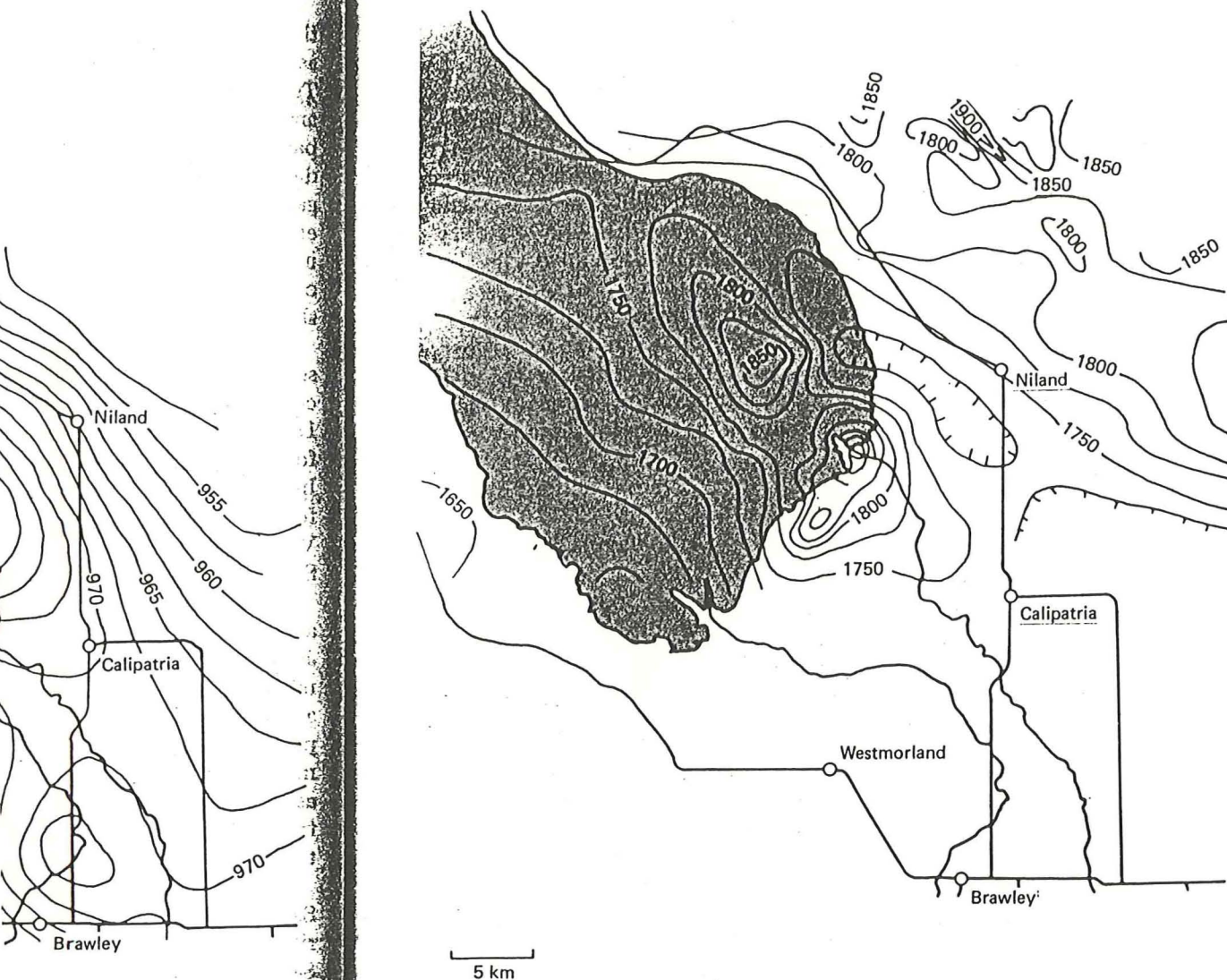


Fig. 8. Aeromagnetic map of the area near the Salton Sea Geothermal Field (after Griscorn and Muffler, 1971). The contour interval is 25 gammas.

the magnetic ridge to be caused by intrusive rocks at depths greater than 2 km and the elliptical anomalies to be a result of dike and sill clusters at depths of approximately 1 km beneath the surface.

Meidav et al. (1976) made a recent resistivity survey in the vicinity of the geothermal field. Electrical currents as high as 200 A were used to detect resistivities of less than 0.5Ω to depths of several kilometres. The survey consisted of 60 soundings with maximum separation of over 5 km and

Salton Sea Geothermal Field
of a seismic refraction profile

Griscom and Muffler
used ones, with the dominant
Calipatria to the middle of
anomalies are superimposed
associated with the volcanic
anomalies. They interpreted

approximately 60 km of dipole survey lines. In these soundings, the deepest layer they could detect was almost always resistive. The total transverse conductance of the overlying layers was calculated from each sounding curve using the method described by Keller and Frischknecht (1966). The conductance value, essentially the sum of the products of conductivity thickness for all the overlying layers, is the most accurately determined quantity for resistivity soundings. A contour map of the conductance determined from the data of Meidav et al. (1976) is seen in Fig. 9. A large volume of the sedimentary

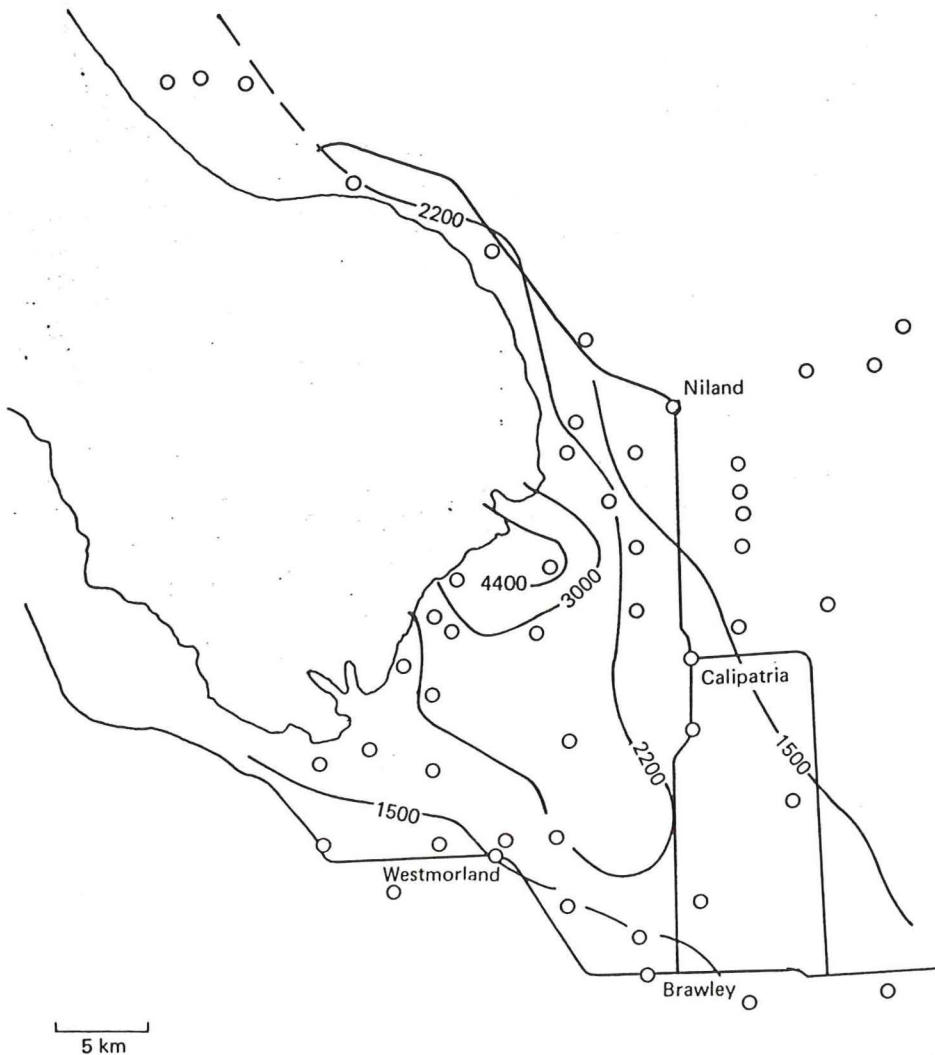


Fig. 9. Conductance map for area near the Salton Sea Geothermal Field (after Kasameyer, 1976). Open circles indicate the location of the soundings. Conductance is in siemens.

rock, located between conductivity and thickness sequence is greatest conductance extends

Low-resistivity zone that is hot or saline, thermal reservoir of the center of the Salton Sea, presumably from because resistivity increases rapidly to the west, a loss of porosity or low resistivity extends extremely low resistivity zone. A cool well located 6 km west of Niland has a resistivity here is inf

Seismic refraction studies

A large-scale survey was conducted and four long-distance profiles were obtained. One interpretation of the seismic data is that the Geothermal Field is located beneath the gravity anomaly. If this profile is correct

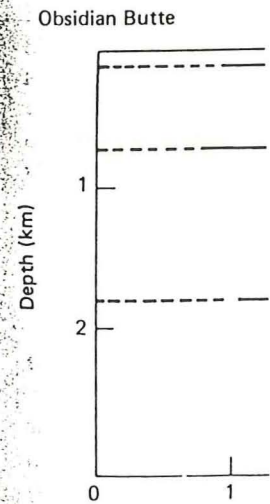


Fig. 10. Seismic refraction profile across the Salton River on the west (after Kasameyer, 1976). V is velocity.

soundings, the deepest
 the total transverse con-
 each sounding curve
 ht (1966). The conduc-
 ductivity thickness for
 ined quantity for resistivi-
 etermined from the data
 ne of the sedimentary

rock, located between the surface and 2 km, is seen as highly conductive. The conductivity and thickness product (conductance) of this sedimentary sequence is greatest in the area of the drilled field, but a broad area of high conductance extends along the axis of the valley (Kasameyer, 1976).

Low-resistivity zones result when porous rocks are saturated with fluid that is hot or saline, or both. Thus the physical boundaries of a porous geothermal reservoir of saline fluid may be determined from resistivity data. In the center of the Salton Sea Geothermal Field, the low resistivity results presumably from both increased temperature and salinity. The resistivity increases rapidly to the northeast and southwest of the known field, indicating a loss of porosity or lower temperature and salinity of the fluid. An area of low resistivity extends southeast from the known geothermal area, and extremely low resistivities ($0.5 \Omega\text{-m}$) were detected in the vicinity of a relatively cool well located 6 km from the Salton Sea Geothermal Field. The low resistivity here is inferred to be the result of saline fluid in high porosity rock.

Seismic refraction survey

A large-scale survey of the field involving seven seismic refraction profiles and four long-distance refraction shots was recently completed (Frith, 1978). One interpretation of data from a seismic profile that crosses the Salton Sea Geothermal Field is shown in Fig. 10. The location of the profile is seen on the gravity anomaly map (Fig. 7).

If this profile is compared with others in the Imperial Valley, an anomalous-

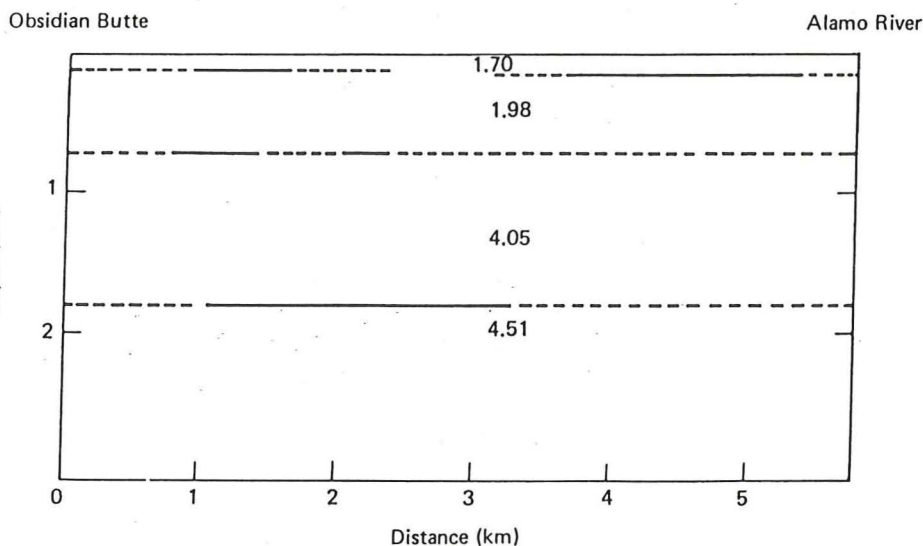
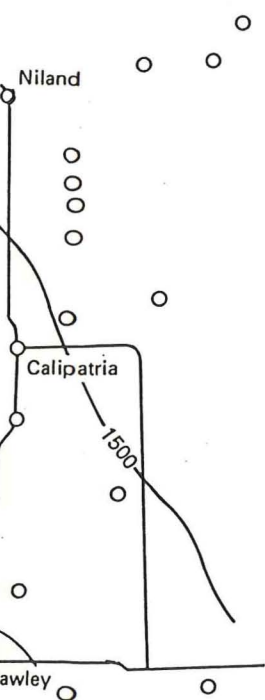


Fig. 10. Seismic refraction profile running from Obsidian Butte on the east to the Alamo River on the west (after Frith, 1978). The position of the profile is indicated on the gravity anomaly map (Fig. 7). Velocities are in km/s.

al Field (after Kasameyer,
 ductance is in siemens.

ly high velocity at shallow depths within the Salton Sea Geothermal Field can be seen. Combs and Hadley (1977) reported a velocity of 2.60 km/s at a depth of 0.9 km for an area near the East Mesa geothermal anomaly, and Biehler et al. (1964) a velocity of 2.71 km/s at a similar depth near Westmorland. The higher velocity of 4.06 km/s in the Salton Sea field at comparable depths probably results from intrusion of basaltic material near the surface or the reduction of sediment porosity with hydrothermal alteration.

Seismicity and inferred faults

The Salton Sea field is located in the offset region between the San Andreas fault and the Brawley fault. As a result, the region is subject to intensive

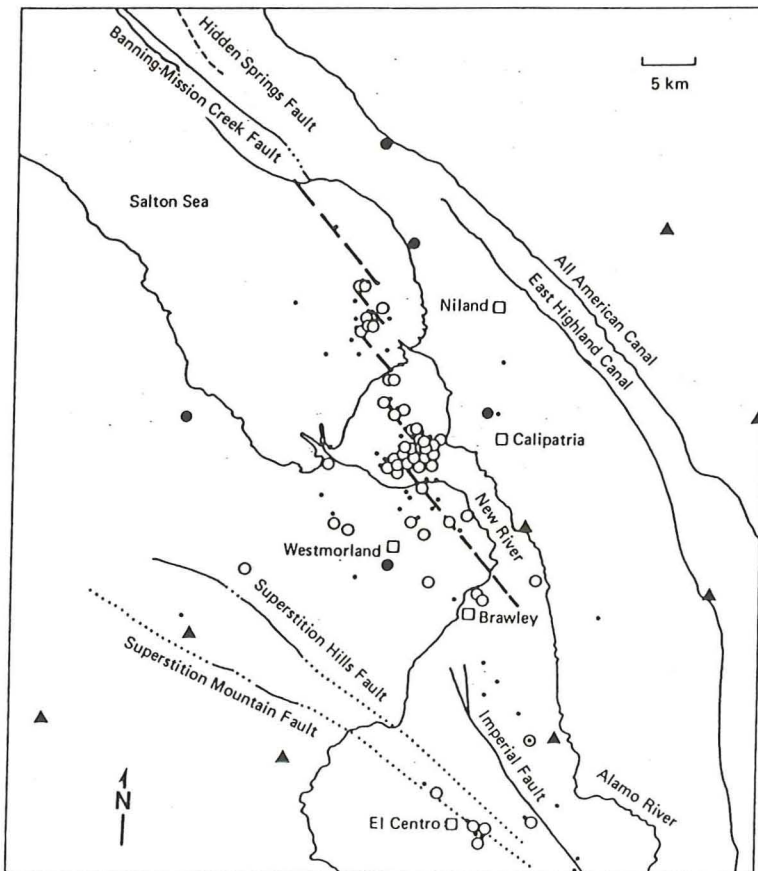


Fig. 11. Location of earthquake epicenters in the Imperial Valley for the period October 1, 1976 through December 31, 1976 (after Schnapp and Fuis, 1977). The solid triangles are seismograph stations in the Imperial Valley network installed in 1973. Solid circles are the seismograph stations installed in November 1976. Open circles and dots are the observed epicenters. Tentative fault locations are shown in broken lines.

seismic activity (Fig. 1). Geophysical and geological data for the field are shown in Fig. 2. The seismic survey (Gilpin and Furgerson, 1972). The (Babcock, 1971) and the (1968). The Red Hill fault, was traced with interpreted from the geophysical data and subsequently located.

THERMAL CHARACTER

Subsurface temperature

Temperature data from (Helgeson, 1968; Ranc and personal communication) surveys the measurements prior to drilling. The distribution of the heat source distribution in the geothermal field.

The equilibrium production and two prominent features in the lower portions of the field, i.e., 200°C higher than 1 km to the south of the field are 140°C higher than the valley. Second, the temperature does not change with depth, the temperature versus distance of heat transfer within the field.

Surface gradient analysis

The equilibrium temperature and the average gradient in the field, in which the gradient is not constant. Surface temperature measurements from geophysical data points from greater depths (see Table 1). Surface temperatures are given by eye. In all cases the average is $23 \pm 1.0^\circ\text{C}$. The uncertainty is $\pm 5^\circ\text{C}$ (one standard deviation).

Nine wells have their

Sea Geothermal Field can
 y of 2.60 km/s at a depth
 anomaly, and Biehler et
 ear Westmorland. The
 comparable depths
 ear the surface or the
 eration.

between the San Andreas
 subject to intensive



y for the period October 1
 7). The solid triangles are
 1973. Solid circles are the
 and dots are the observed

seismic activity (Fig. 11) (Schnapp and Fuis, 1977). Faults were identified by geophysical and geological techniques, and their locations in the geothermal field are shown in Fig. 1. The Brawley fault zone was identified by a portable seismic survey (Gilpin and Lee, 1978) and a resistivity survey (Meidav and Furgerson, 1972). The Calipatria fault was identified using infrared detection (Babcock, 1971) and the alignment of thermal hot springs (Muffler and White, 1968). The Red Hill fault, located between the Brawley and the Calipatria faults, was traced with correlations derived from electric logs (Towse, 1975), interpreted from the ground magnetic survey (Meidav and Furgerson, 1972), and subsequently located with a seismic refraction survey (Frith, 1978).

THERMAL CHARACTERISTICS OF THE SALTON SEA GEOTHERMAL FIELD

Subsurface temperature data

Temperature data from the deep wells in the Salton Sea Geothermal Field (Helgeson, 1968; Randall, 1974; Palmer, 1975; Magma Power Company, personal communication, 1979) were critically analyzed to determine in which surveys the measurements represent equilibrium temperatures that existed prior to drilling. The data in those surveys were used to gain insight into both the heat source distribution, and the mechanisms of heat transfer within the geothermal field.

The equilibrium profiles for 13 wells within the field are shown in Fig. 12, and two prominent features are evident. First, the field temperatures are high in the lower portions of the profiles. At 2 km they are typically over 320°C, i.e., 200°C higher than at a similar depth in the Wilson No. 1 well, which is 15 km to the south of the field and in a nongeothermal area. Also, temperatures are 140°C higher than those reported in other geothermal fields within the valley. Second, the thermal gradient in the upper part of most of the wells does not change with depth. We can infer from this the general character of the temperature versus depth curve at any location and understand the control of heat transfer within the geothermal system.

Surface gradient analysis for deep wells

The equilibrium temperature profiles discussed above were used to estimate the average gradient in the near-surface conductive zone and the depth to which the gradient is nearly constant. For wells with enough data, the near-surface temperature measurements were fitted with a straight line. Additional data points from greater depths were added until the fit failed a chi-square test (see Table 1). Surface gradients for wells with few data points were estimated by eye. In all cases the average annual surface temperature was assumed to be $23 \pm 1.0^\circ\text{C}$. The uncertainty for a single temperature measurement is assumed to be $\pm 5^\circ\text{C}$ (one standard deviation, σ) unless stated otherwise.

Nine wells have thermal gradients with similar characteristics and configura-

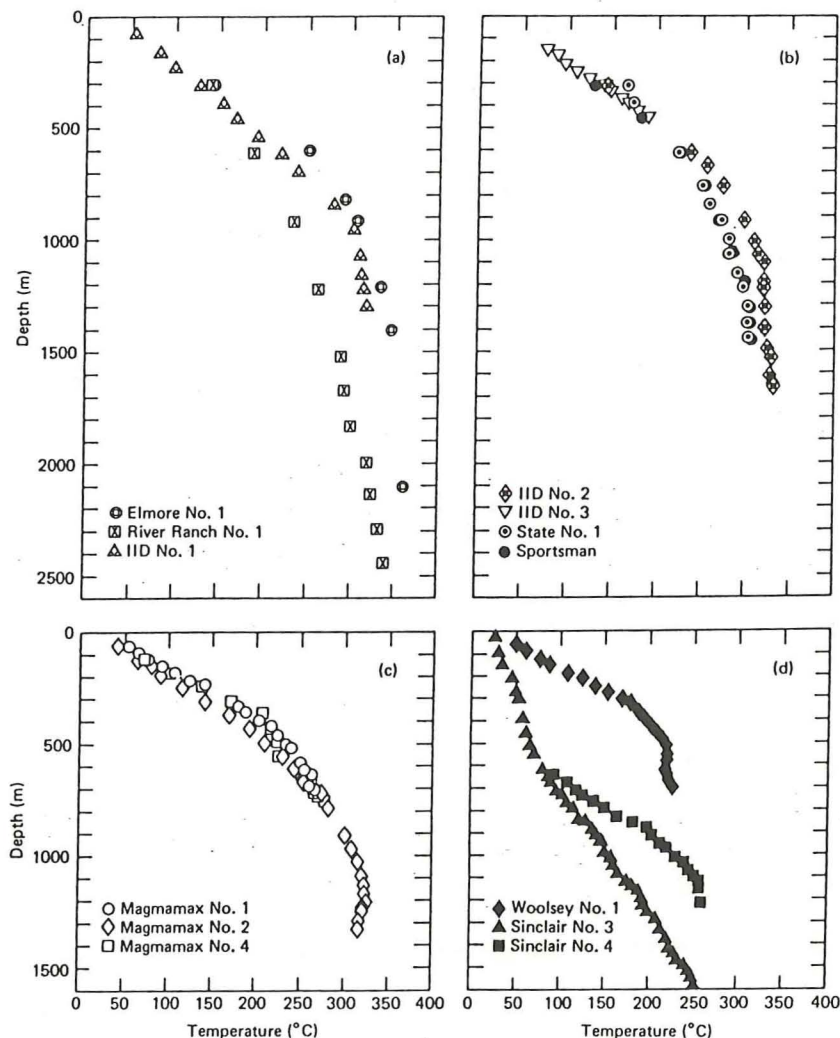


Fig. 12. Equilibrium temperature profiles for 13 wells in the Salton Sea Geothermal Field. (a), (b) Wells from the northern part of the field. (c), (d) Wells from the southern part of the field. The data for these profiles are from Helgeson, 1968; Randall, 1974; Palmer, 1975; and Magma Power Company (personal communication, 1979).

tions. The gradients are high in the upper portions of the wells ($0.38^{\circ}\text{C}/\text{m}$, $1\sigma = 0.05^{\circ}\text{C}/\text{m}$) and are low and nearly constant at greater depths. **The transition in the character of the gradient occurs in reservoir rocks beneath the impermeable cap.**

Four wells have thermal profiles significantly different from the profiles described above. In Magmamax No. 4, the high gradient at the surface increases slightly (but significantly) with depth in the impermeable cap. In

TABLE 1

Near-surface temperature
Geothermal Field, a

Well

River Ranch No. 1
IID No. 1
IID No. 2
IID No. 3
State No. 1^b
Elmore No. 1
Magmamax No. 1
Magmamax No. 2

Magmamax No. 3^c
Magmamax No. 4^d

Woolsey No. 1

Sinclair No. 3
Sinclair No. 4
Sportsman

^aGradient estimated:

^bState No. 1. Data versus depth.

Best fit and standard deviation.

^cThe data set represents the average gradient

from Magmamax No. 3.

^dThe gradient increases with depth.

The average gradient is $0.38^{\circ}\text{C}/\text{m}$.

River Ranch No. 1

to suggest a gradual

temperature holes

The proximity of the

suggests that the geothermal

the two Sinclair wells

increases with depth

The general mechanism

inferred from these

the cap is uniform in

profiles, the vertical

uniform and the horizontal

presence of convective

No. 1). Furthermore

on the lithologic cap

TABLE 1

Near-surface temperature gradient associated with geothermal wells in the Salton Sea Geothermal Field, and the maximum depth to which the gradient is valid

Well	Gradient (°C/m)	Maximum depth, <i>D</i> , of valid gradient (m)	Comments
River Ranch No. 1	< 0.4	$D < 300$	may be 1.6°C/m
IID No. 1	0.316 ± 0.007^a	$700 < D < 850$	
IID No. 2	0.39 ± 0.02	$D < 300$	based on two points
IID No. 3	0.366 ± 0.006^a	$460 < D$	
State No. 1 ^b	0.40 ± 0.05^a	$300 < D < 600$	
Elmore No. 1	0.391 ± 0.008^a	$600 < D < 650$	
Magmamax No. 1	0.457 ± 0.009^a	$460 < D < 525$	three data sets, 1972
Magmamax No. 2	0.368 ± 0.008^a	$570 < D < 650$	three data sets, 1974–1976
Magmamax No. 3 ^c			
Magmamax No. 4 ^d	0.350 ± 0.04^a	$120 < D < 180$	six data sets, 1973–1976
Woolsey No. 1	0.463 ± 0.010^a	$400 < D < 430$	three data sets, 1974–1976
Sinclair No. 3	0.11 ± 0.007	$D \sim 690$	
Sinclair No. 4	< 0.11	$D < 650$	based on two points
Sportsman	0.337 ± 0.007^a	$600 < D < 750$	

^aGradient estimated from statistical analysis.

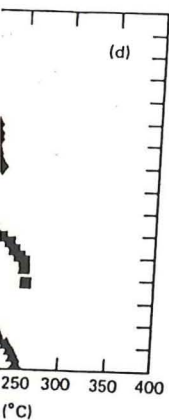
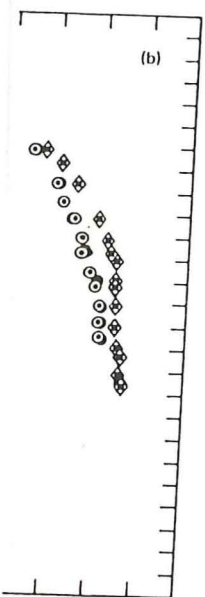
^bState No. 1. Data variability greatly exceeds uncertainty of $\pm 5^\circ\text{C/m}$ in shallow zones. Best fit and standard deviation were determined subjectively.

^cThe data set representing equilibrium temperatures cannot be determined. The gradient from Magmamax No. 4 was used.

^dThe gradient increases to 0.58°C/m and is constant for depth ranging from 150 to 350 m. The average gradient from 0 to 350 m is 0.49°C/m .

River Ranch No. 1, three measurements in the impermeable cap provide data to suggest a gradual decrease in gradient with depth. However, nearby shallow temperature holes (Lee and Cohen, 1977) indicate a very high local gradient. The proximity of this well to active mud volcanoes and the shallow CO_2 field suggests that the geotherm here is strongly distorted by shallow fluid flow. In the two Sinclair wells, the near-surface gradient is low and constant and increases with depth below the impermeable cap.

The general mechanism of heat transport within the lithologic cap can be inferred from these observations. If we assume that thermal conductivity in the cap is uniform in the area determined by the nine wells with similar profiles, the vertically conducted heat flow within the lithologic cap is nearly uniform and the horizontally conducted heat flow negligible. There is no evidence of convective heat flow in the lithologic cap (except near River Ranch No. 1). Furthermore, near these nine wells the thermal boundary conditions on the lithologic cap must have been constant for a sufficiently long time to



Salton Sea Geothermal Field.
from the southern part of the
all, 1974; Palmer, 1975;

the wells (0.38°C/m ,
ter depths. The transi-
rocks beneath the

t from the profiles
at the surface in-
ermeable cap. In

enable the conductive heat flow to equilibrate to steady state over a large area and to a great depth.

Because steady-state conduction is the dominating heat transfer mechanism in the lithologic cap, we can use shallow thermal holes to determine the gradient of the thermal profile throughout the lithologic cap where deep wells do not exist.

If the subsurface temperature data are compared with the surface gradient analyses, it is possible to arrive at a composite picture of the thermal anomaly. At any location, the temperature versus depth profile down to 2000 m can be described as one of the following:

(A) A nearly constant conductive vertical heat flow in the upper few hundred metres and a nearly isothermal zone at depth. The surface gradient is moderately high, around $0.4^{\circ}\text{C}/\text{m}$.

(B) Nearly constant heat flow with a value consistent with the normal regional gradient. In these areas the surface gradient is much lower, around $0.1^{\circ}\text{C}/\text{m}$.

(C) An intermediate region with a low near-surface gradient and an increasing temperature gradient at greater depths.

The distribution of wells based on the descriptions above, is shown in Fig. 13. The data available for shallow wells do not enable us to distinguish descriptions (B) and (C). Therefore, all shallow wells are labeled either "a" or "b". Those with observed gradients greater than $0.35^{\circ}\text{C}/\text{m}$ are labeled "a" and those less than $0.16^{\circ}\text{C}/\text{m}$, "b".

Interpreted boundaries define regions containing wells with temperature profiles of similar character. The region with wells labeled "A" (uniform, moderately high gradient) is elliptical and covers most of the Salton Sea Geothermal Field. Its major axis strikes across the axis of the Salton Trough and is 8–12 km in length. The length of the minor axis is unknown because there are no measurements in the Salton Sea. The region containing wells labeled "C" (transition) includes only the two deep Sinclair wells but is assumed to surround the first region, "A". The region with wells labeled "B" lies outside the others.

The near-surface gradient can be used to infer the boundaries of the area of high heat flow. However, the gradient cannot be used successfully to predict temperature differences at depth within the field (see Fig. 14). To predict the temperature at depth, we must determine variations in thickness of the steady-state conduction zone. The thermal profiles from deep wells were also analyzed to determine what geologic factors control this thickness and to predict the temperature at depth in areas where there are no deep wells.

Vertical heat transport

The temperature gradient in wells within the central portion of the anomaly is dramatically reduced at a depth of approximately 500 m, and this is

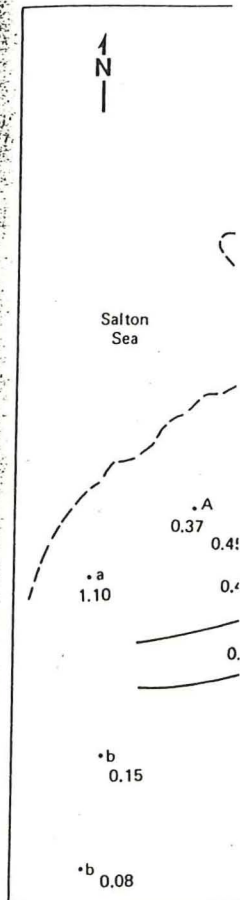


Fig. 13. A map of the is represented by three surface gradient, and a curve. Upper case letter uniform heat flow in the Wells marked "B" have marked "C" have low Lower case letters represent characteristics. Holes in shallow wells are not shown. Lines represent the appropriate "A", "B", or "C".

presumed to mark a region is characterized lower by low gradient the cap long enough heat transfer mechanisms. We refer to the

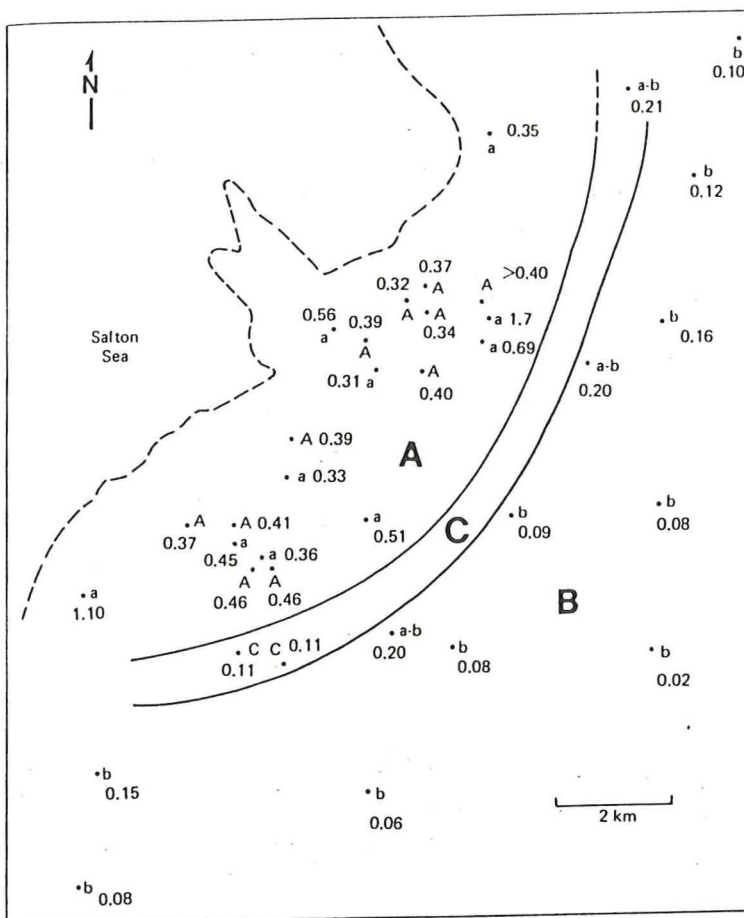


Fig. 13. A map of the spatial character of the geothermal anomaly. Each measurement point is represented by three symbols: a dot showing the location, a number indicating the near-surface gradient, and a letter representing the character of the temperature versus depth curve. Upper case letters indicate deep wells. Wells marked "A" have a moderately high uniform heat flow in the upper few hundred metres, and a nearly isothermal zone at depth. Wells marked "B" have a nearly constant low heat flow throughout their depth. Wells marked "C" have low heat flow near the surface, but their gradient increases with depth. Lower case letters represent shallow hole data (Lee and Cohen, 1977) with corresponding characteristics. Holes marked "a" or "b" have high or low gradients, respectively. The shallow wells are not deep enough to distinguish between "B" and "C" behavior. The solid lines represent the approximate boundaries of regions with similar characteristics, indicated by "A", "B", or "C".

presumed to mark a change in the major mode of heat transport. The upper region is characterized by steep gradients and heat flow by conduction and the lower by low gradients that, however, must have been supplying heat to the cap long enough for steady-state conduction to develop. The dominant heat transfer mechanism in the lower region must be convective flow of pore fluids. We refer to this region as the convective zone.

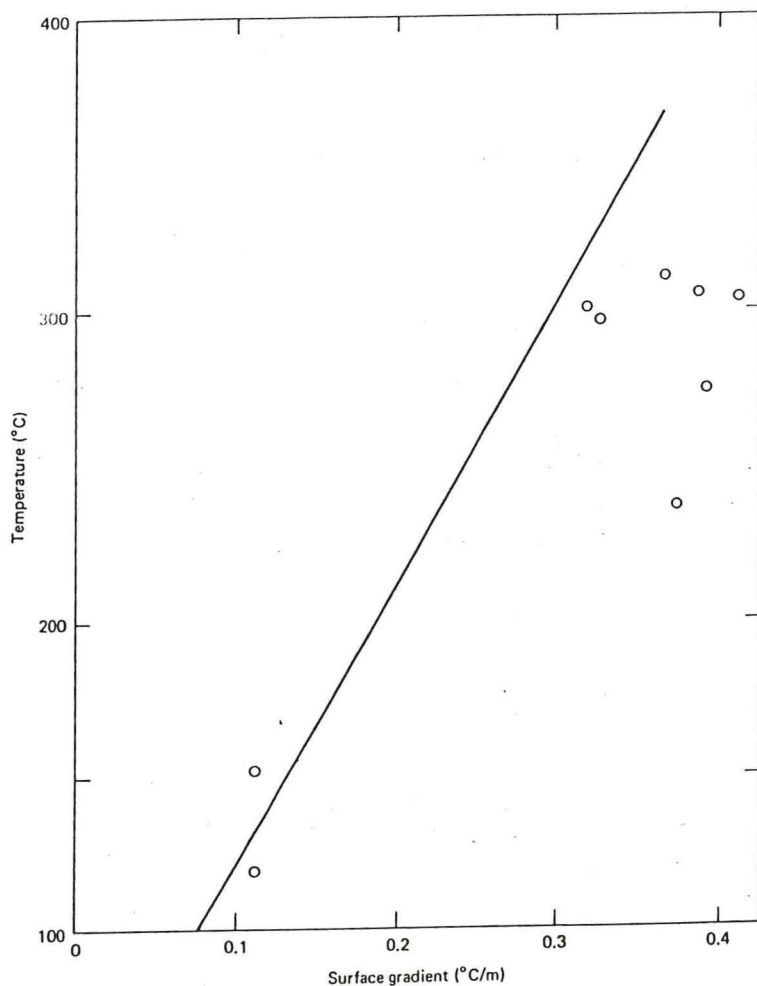


Fig. 14. Surface gradient versus temperature at a depth of 1000 m for 9 wells in the Salton Sea Geothermal Field. The line represents the temperature that would be at 1000 m if the gradient were constant.

Previous authors (Dutcher et al., 1972; White, 1968) suggested that vertical heat transport in the Salton Sea field is by large-scale convection cells encompassing the entire section of permeable reservoir rocks. We propose a method to determine the thickness of the zone where conductive heat flow dominates and use it to show that the zone includes a portion of the uppermost section of reservoir rocks immediately beneath the cap rock. Our results suggest the existence of a thermal cap in the Salton Sea field that is thicker in some places than the impermeable lithologic cap described earlier. In addition, we find evidence indicating that thin shale beds impede vertical fluid flow and the amount of convective heat transport in a section is controlled primarily by the thickness

of sand beds. Co- place within that If most of the duction, the heat ΔZ) should vary material, κ , i.e.,

$$Q_{\text{cond}} = \kappa \frac{\Delta T}{\Delta Z} = c$$

If we determine l the lower bound:

The relative cc ing simplifying as:

(1) The lithologic stone or pure shale correct the gradient anhydrite rich layers temperature gradients, this simplification

(2) The thermal ature and pressure

(3) The conductivity is measured

If a well interval κ_i , and thickness ΔZ_i is ΔT_i , then the

$$Q_{\text{cond}} = \frac{\Delta T}{\Delta Z} \left(\frac{1}{\Delta Z} \right)$$

If each layer is either and ΔZ_s is the sum

$$Q_{\text{cond}} = \frac{\Delta T}{\Delta Z} \left[\frac{1}{\Delta Z} \right]$$

and:

$$Q_{\text{cond}} = \frac{\Delta T}{\Delta Z} \left[\frac{\Delta Z_i}{\Delta Z} \right]$$

$$\frac{Q_{\text{cond}}}{\kappa_{\text{sh}}} = \frac{\Delta T}{\Delta Z} \cdot \frac{1}{1 + \alpha}$$

where $\alpha = \kappa_{\text{sh}}/\kappa_{\text{sa}}$

of sand beds. Consequently, large-scale vertical convection of fluid cannot take place within that part of the reservoir penetrated by wells.

If most of the heat in the thermal cap is transported by steady-state conduction, the heat flow, Q_{cond} , is constant, and the temperature gradient ($\Delta T/\Delta Z$) should vary in the cap inversely with the thermal conductivity of the material, κ , i.e.,

$$Q_{\text{cond}} = \kappa \frac{\Delta T}{\Delta Z} = \text{constant} \quad (1)$$

If we determine how deep in the reservoir this relationship holds, we can define the lower boundary of the thermal cap.

The relative conductive heat flow at any depth is estimated using the following simplifying assumptions:

(1) The lithology consists of infinite horizontal slabs of either pure sandstone or pure shale, as deduced from the electric logs. The analysis does not correct the gradient in the lower lithologic cap for the presence of the anhydrite rich layers. Although it is possible to locally correlate changes in temperature gradient with the presence of massive anhydrite in the cutting samples, this simplification will not affect the estimates of thermal cap thickness.

(2) The thermal conductivity in either rock type is independent of temperature and pressure.

(3) The conductive heat flow is constant between depths where temperature is measured.

If a well interval of length ΔZ consists of n layers with thermal conductivity κ_i , and thickness h_i , $i = 1, \dots, n$, and the temperature difference over that interval is ΔT , then the conductive heat flow, Q , is given by:

$$Q_{\text{cond}} = \frac{\Delta T}{\Delta Z} \left(\frac{1}{\Delta Z} \cdot \sum_{i=1}^n \frac{h_i}{\kappa_i} \right)^{-1} \quad (2)$$

If each layer is either sand or shale, with conductivity κ_s or κ_{sh} respectively, and ΔZ_s is the sum of the thicknesses of the sand layers, then:

$$Q_{\text{cond}} = \frac{\Delta T}{\Delta Z} \left[\frac{1}{\Delta Z} \cdot \left(\sum_{\text{sand}} \frac{h_i}{\kappa_s} + \sum_{\text{shale}} \frac{h_i}{\kappa_{\text{sh}}} \right) \right]^{-1} \quad (3)$$

and:

$$Q_{\text{cond}} = \frac{\Delta T}{\Delta Z} \left[\frac{\Delta Z_s}{\Delta Z \kappa_s} + \left(1 - \frac{\Delta Z_s}{\Delta Z} \right) \cdot \frac{1}{\kappa_{\text{sh}}} \right]^{-1} \quad (4)$$

$$\frac{Q_{\text{cond}}}{\kappa_{\text{sh}}} = \frac{\Delta T}{\Delta Z} \cdot \frac{1}{1 + (\alpha - 1)R} = \text{relative conductive heat flow} \quad (5)$$

where $\alpha = \kappa_{\text{sh}}/\kappa_s$ and $R = \text{sand percentage}$.

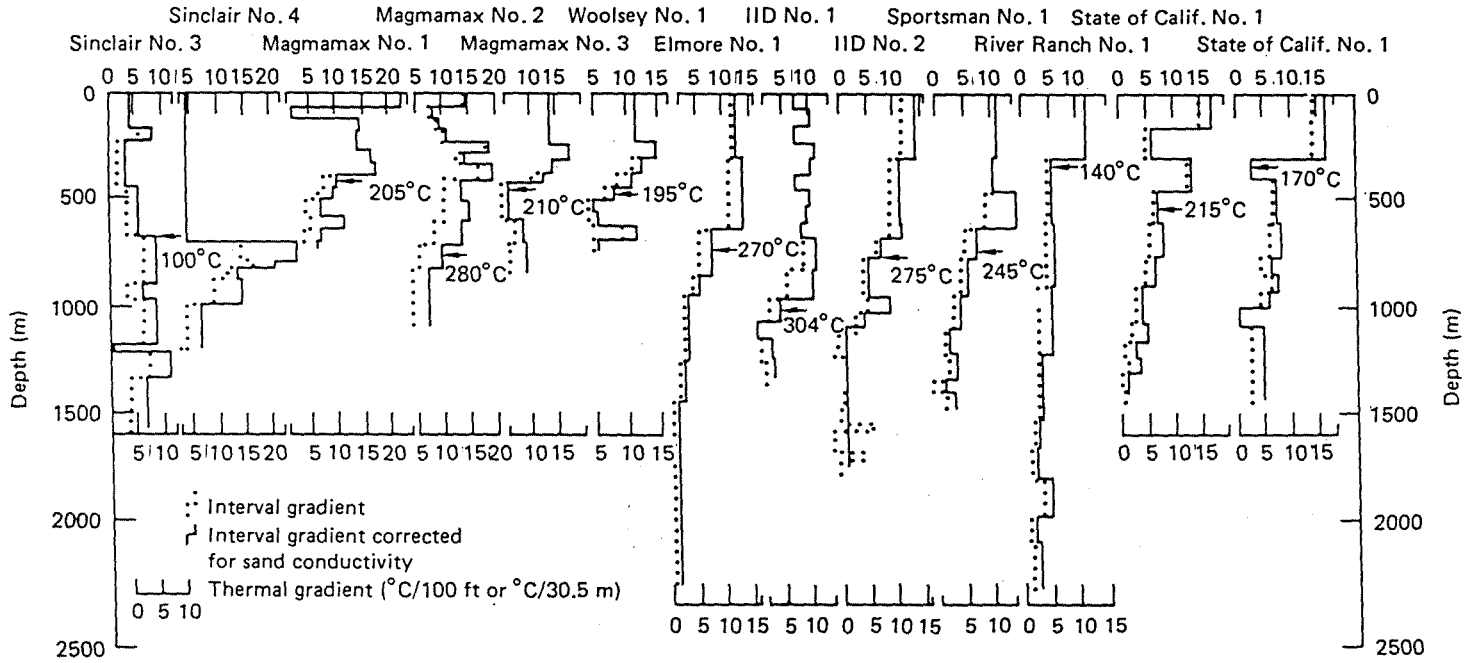


Fig. 15. Thermal gradients versus depth for 12 wells in the Salton Sea Geothermal Field. The interval gradient is indicated by a dashed line. The gradient corrected for the sand conductivity is indicated by a solid line. The depths at which the conductive heat flow has decreased by 30 to 40% are indicated by arrows. Convection is interpreted as a mechanism for significant heat transfer below these points. If the decrease in conductive heat flow occurs between widely-spaced temperature measurements, the arrow is placed at a change of lithology between the observation depths. The depth uncertainty is greater than 30 m in all cases. The data for State of California No. 1 are (left) from the State of California Division of Oil and Gas and (right) from Helgeson (1968).

The relative co
 (Fig. 15). The cor
 most wells and th
 Convection is in
 the level where th
 ness of the thermi
 at adjacent wells t
 consistent with th
 mamax No. 3, anc
 depths shown in F
 thermal cap is, in t
 upper portion of t
 conduction, despit
 ments.

A comparison o
 16) suggests that c
 shown at depths fr
 zero gradients exis

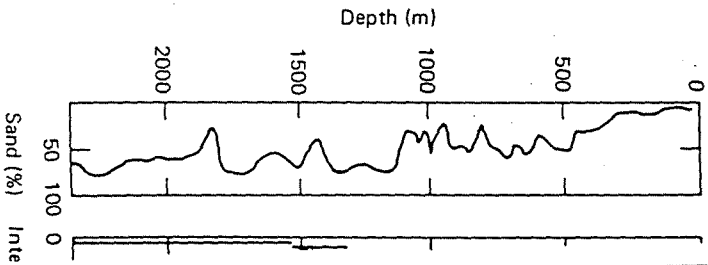


Fig. 16. The percentage of sand versus depth in the Salton Sea Geothermal field.

Fig. 15. Thermal gradients versus depth for 12 wells in the Salton Sea Geothermal Field. The interval gradient is indicated by a dashed line. The gradient corrected for the sand conductivity is indicated by a solid line. The depths at which the conductive heat flow has decreased by 30 to 40% are indicated by arrows. Convection is interpreted as a mechanism for significant heat transfer below these points. If the decrease in conductive heat flow occurs between widely-spaced temperature measurements, the arrow is placed at a change of lithology between the observation depths. The depth uncertainty is greater than 30 m in all cases. The data for State of California No. 1 are (left) from the State of California Division of Oil and Gas and (right) from Helgeson (1968).

The relative conductive heat flow for 12 wells changes as a function of depth (Fig. 15). The conductive heat flow is nearly constant in the upper section of most wells and then decreases rapidly with increasing depth.

Convection is inferred to be the important mechanism of heat flow below the level where the conductive heat flow decreases. An estimate of the thickness of the thermal cap is provided in Fig. 15. The depth differs considerably at adjacent wells but becomes increasingly shallow away from the Salton Sea, consistent with the westward dip of the reservoir strata. The Sinclair, Magmamax No. 3, and River Ranch wells appear to be anomalous. If we compare the depths shown in Fig. 15 with previous lithologic observations, we see that the thermal cap is, in general, somewhat thicker than the lithologic cap, and the upper portion of the clastic sediments appears to transfer heat largely through conduction, despite the inferred high porosity and permeability of the sediments.

A comparison of well logs and temperature gradients for Elmore No. 1 (Fig. 16) suggests that convection is lithology controlled. Modest gradients are shown at depths from 500 to 1000 m in the zone of thin sand beds, but near zero gradients exist below 1400 m where sand beds are thick.

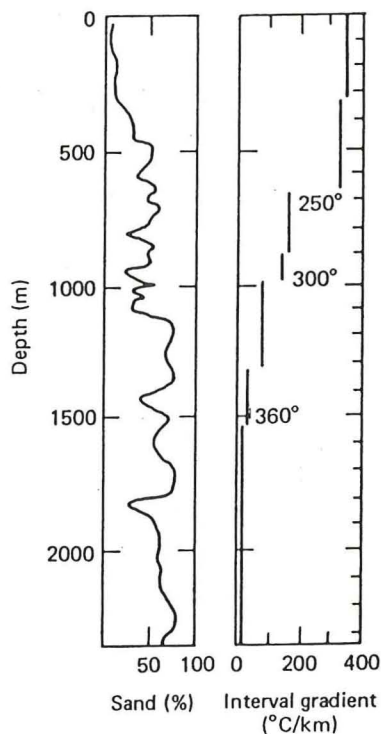


Fig. 16. The percentage of sand and the interval gradients for the Elmore No. 1 well in the Salton Sea Geothermal Field.

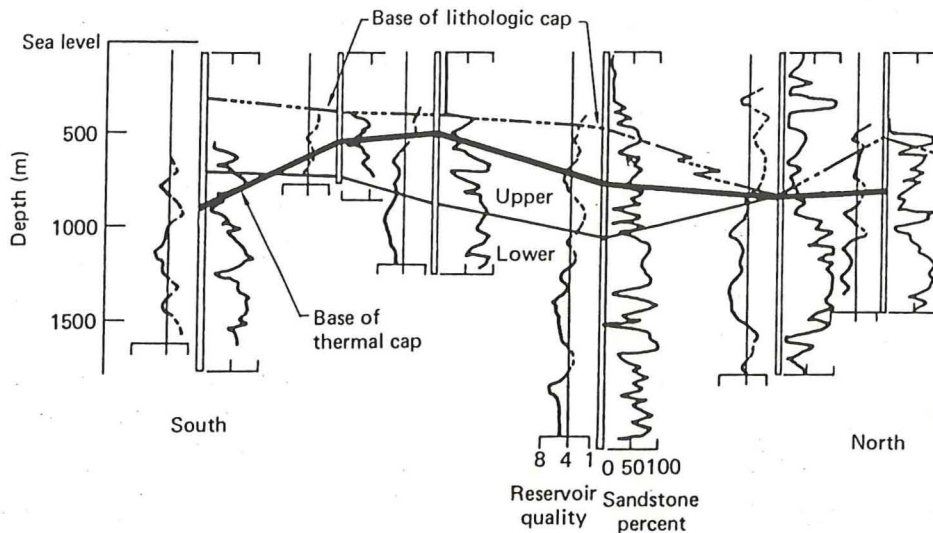


Fig. 17. A north-south section across the Salton Sea Geothermal Field showing that the thermal cap does not coincide with the lithologic cap. Sandstone percentage, a subjective measure of reservoir quality (Towse, 1975), and the thickness of the base of the thermal cap are shown for six wells. From south to north, the wells are Sinclair No. 4, Woolsey No. 1, Magmamax No. 3, Elmore No. 1, IID No. 2, and Sportsman No. 1.

We plotted a north-south cross section and compared the reservoir character with the thickness of the thermal cap (Fig. 17). Towse and Palmer (1975) provided the estimate of reservoir quality based on an interpretation of inferred permeability and continuity of rock units. Two observations are important. First, in all the wells the base of the thermal cap is within the zone where the percentage of sand is high (> 20%). Second, in several wells (Magmamax No. 3, Elmore No. 1, IID No. 2, and Sportsman No. 1) the base of the thermal cap coincides with the first appearance of high reservoir quality (≥ 4). These observations support the idea of lithologic control of heat transport mechanisms within the reservoir. The dominant controls are probably sand bed thickness and lateral continuity of intervening shale beds, although the fracture permeability of shales may be locally significant.

Vertical convection does not occur in some permeable sand zones indicating that vertical permeability is small in the upper part of the section. Several lines of evidence also suggest that individual shale beds can effectively reduce the vertical permeability and thereby prevent large-scale convection cells within the zone of convective flow. Towse and Palmer (1976) and Tewhey (1977) identified several major shale beds over 14 m thick in the reservoir sands which would surely provide impermeable barriers to convective flow if they are not extensively fractured.

Kendall (1976) provides support for the concept of a reservoir split into several hydrologic systems. She found that extensive oxygen and carbon isotope

exchange occurred. Several isotope inversions and correlations suggest that the exchange is largely lateral and that the 900 m indicates the result of the extent of the exchange. The exchange has approximately the same thickness in the wall rocks, indicating that water transport is important.

More evidence for lateral exchange is provided by the fact that, before, no large-scale convection cells were observed in the wells, and well profiles in the field observation preclude large-scale convection (Helgeson (1968), and the uncertainty in the analysis of well intercommunication across the field is a measure of permeability in the field.

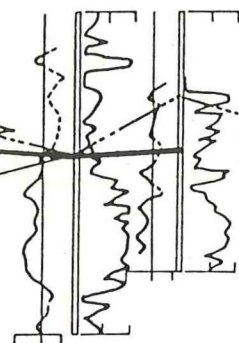
An analysis of the field data supports the hypothesis of vertical convection in individual wells. Numerical and experimental work have found that the heat transfer is controlled by the Rayleigh number, :

$$\eta = \frac{\kappa \alpha \Delta T g H}{\kappa_m \nu}$$

where κ = permeability of the fluid, g = absolute gravity, α = coefficient of the saturated medium, H = thickness of the layer, ν = kinematic viscosity.

To determine a critical Rayleigh number for a given thickness, permeability, and coefficient of the convecting fluid, a series of experiments were investigated. Convective flow was observed for a range of parameters changes and the critical Rayleigh number increases. By a given thickness and permeability, the critical Rayleigh number is buried to a depth where the convective flow is observed.

For this report, the critical Rayleigh number for the reservoir sands are quartzite and sandstone.



North

field showing that the percentage, a subjective at the base of the thermal well No. 4, Woolsey No. 1.

the reservoir character and Palmer (1975) interpretation of observations are important within the zone where wells (Magmamax at the base of the thermal well ≥ 4). These transport mechanisms probably sand bed thickness through the fracture

sand zones indicating section. Several lines actively reduce the convection cells within the well (1977) identify sands which flow if they are not

reservoir split into sand and carbon isotopes

exchange occurred between geothermal brines and reservoir rock and that several isotope inversions can be correlated with stratigraphic horizons. This correlation suggests that water transport in the interval between 300 and 900 m is largely lateral and stratigraphically controlled. Consistent composition below 900 m indicates that the water there is more thoroughly mixed, perhaps as a result of the extensive fractures. In addition, minerals in the larger fractures have approximately the same chemical and isotopic compositions as minerals in the wall rocks, indicating that the large fractures were not major avenues of water transport.

More evidence for a lack of large-scale vertical transport of fluids and, therefore, no large-scale convection cells comes from pressure measurements within the wells, and well interference tests. The hydrostatic pressure-versus-depth profile in the field is consistent with a constant fluid density of 1 g/cm^3 . This observation precludes large convective movements, but, as was pointed out by Helgeson (1968), smaller convection geometries cannot be tested because of the uncertainty in the pressure measurements. Morse and Thorsen (1978) analyzed well interference data and noted that wells 7 m apart did not communicate across a major shale break. They concluded that the vertical permeability in the region is very low.

An analysis of the conditions required for convection in a porous medium supports the hypothesis that the vertical heat transport could result from convection in individual sand layers (at least in the upper reservoir). Elder (1967) did numerical and experimental studies of convection in a porous medium. He found that the heat transport within a single layer is controlled by a modified Rayleigh number, η , and convection only occurs if η is greater than 40.

$$\eta = \frac{\kappa \alpha \Delta T g H}{\kappa_m \nu} \quad (6)$$

where κ = permeability of the layer, α = coefficient of volume expansion of the fluid, g = absolute value of acceleration due to gravity, κ_m = thermal diffusivity of the saturated medium, ν = kinematic viscosity of the convecting fluid, H = thickness of the layer, and ΔT = temperature contrast across the layer.

To determine accurately whether convection will develop in a sand of a given thickness, permeability, and depth, the variation of physical properties of the convecting fluid as a function of temperature and pressure must be investigated. Convection depends strongly on the coefficient of expansion, kinematic viscosity, and the thermal diffusivity of the saturated medium, each highly dependent on temperature. The (conjugate) variation of these three parameters changes η and makes convection much stronger when the temperature increases. By considering this variation, we can show that sand units of a given thickness and permeability are more likely to support convection if buried to a depth where the temperature was high.

For this report, we assumed the convecting fluid is pure water and the reservoir sands are quartzitic sandstones. The permeability in upper reservoir rocks

was estimated to be 500 md, and permeability in lower reservoir rocks was estimated to be 180 md (Morse and Thorsen, 1978).

Using Elder's criterion for η , we prepared tables in which the thickness of sand necessary for convection is given as a function of permeability, temperature, and geothermal gradient. In Table 2 is the required thickness as a function of temperature for two geothermal gradients and permeabilities of 180 md, representative of the lower reservoir, and 500 md, representative of the upper reservoir. We chose the geothermal gradients to represent the range of possible gradients before convection starts.

TABLE 2

Thickness necessary to support convection

Assumed temperature (°C)	Necessary thickness at assumed gradients			
	permeability of 180 md		permeability of 500 md	
	0.33°C/m (m)	0.16°C/m (m)	0.33°C/m (m)	0.16°C/m (m)
0	1385	1992	832	1195
50	474	681	284	408
100	247	355	148	213
150	157	225	94	135
200	107	154	64	92
250	78	112	47	67
300	52	75	31	45

Three major points emerge from the analysis. First, temperature is a very important parameter. Given a permeability of 500 md and a gradient of 0.33°C/m, it would require a bed 284 m thick to convect at 50°C, but at 300°C, a bed 31 m thick would support convection. Even under a high temperature gradient and high permeability, a sand unit would have to be thicker than 60 m to support convection at temperatures less than 200°C. Second, in the upper reservoir, convection probably occurs in individual sand units. Temperatures greater than 200°C will produce convection in sand units varying in thickness from 30 to 100 m, depending on the geothermal gradient. Finally in the lower reservoir, convection is unlikely in individual sand units because of their lower permeability. Under high geothermal gradients and at 200°C, a sand unit must be 107 m thick for convection to occur. This approaches the upper limit of thickness for a sand bed in the Salton Sea Geothermal Field. Therefore, we would expect fracture permeability to be the dominant factor facilitating convection in deep reservoir rocks.

Horizontal heat transport within the reservoir

It is possible that a much larger scale of horizontal convection is superim-

posed on the small-scale convection in the reservoir. The segmented vertical fractures (Fig. 18) support the flow of fluid out the area. This is more than the vertical,

Magmamax No. 3 —
Woolsey No. 1 —
Sinclair No. 3 —
Sinclair No. 4 —

Fig. 18. Data from S (after Chan and Tew) and the logs were dis

If the temperature is a function of thickness, it is a nearly straight line to a horizontal flow. The geothermal field is constant for the field. This is a rough index of the base of the cap rock source of the heat to the base of the field of large-scale horizontal localized heat sources to the impermeable. If this is correct, then this will be the total mass of paper we will modify to compare it with models within the field.

reservoir rocks was

which the thickness of permeability, temperature, and thickness as a function of depth. The permeabilities of 180 md, representative of the upper part of the range of possible

md

/m

temperature is a very high gradient of about 50°C, but at 200°C. Second, in the sand units. Temperature units varying in gradient. Finally, sand units because of the high salinity brine and at 200°C, a dominant factor

convection is superimposed

posed on the small-scale convection, which controls the vertical heat transport in the reservoir. High lateral permeability occurs even where the reservoir is segmented vertically by shale beds. SP logs of 350-ft (100-m) intervals from nine geothermal wells placed in juxtaposition to emphasize similarities (Fig. 18) support the idea of widespread continuity of individual sand beds throughout the area. Thus, the lateral permeability within the reservoir is much greater than the vertical, and the possibility of large-scale lateral flow exists.

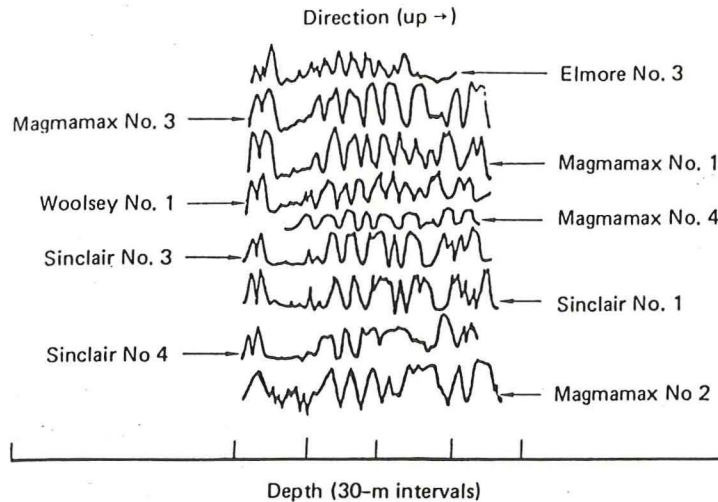


Fig. 18. Data from SP logs of nine geothermal wells with markers set at 100-m intervals (after Chan and Tewhey, 1977). The marker bed occurs at a different depth in each well, and the logs were displaced vertically so that similarities among wells can be seen.

If the temperature at the base of the thermal cap in several wells is plotted as a function of the value of the magnetic anomaly at each well head, the result is a nearly straight line (Fig. 19). This unlikely correlation lends further support to a horizontal flow model. The magnetic anomaly at the Salton Sea Geothermal Field is caused by intrusions, which are probably the source of heat for the field. Therefore, the value of the magnetic anomaly can be used as a rough index of the distance from the source of heat. The temperature at the base of the cap apparently decreases monotonically with distance from the source of the heat (Fig. 19), and this is surprising if we consider that the depth to the base of the cap is quite irregular. However, it is consistent with a model of large-scale horizontal flow beneath the lithologic cap. Fluid rises above a localized heat source and spreads laterally away from the source losing heat to the impermeable cap rock. If this model of predominantly horizontal flow is correct, then the high salinity brine inferred from the resistivity data could be the total mass of water that has flowed through the system. In our next paper we will model the heat transport associated with this lateral flow, and compare it with more detailed observations on the temperature distribution within the field.

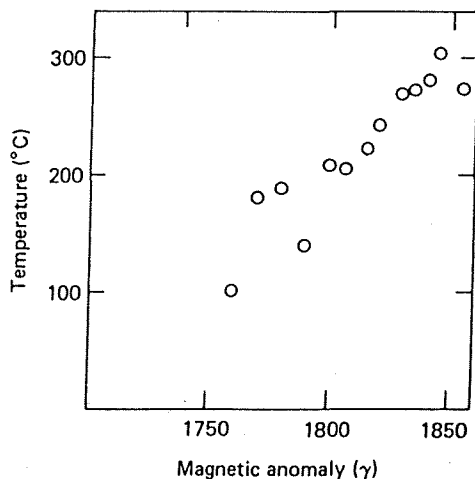


Fig. 19. A cross plot of temperature at the base of the thermal cap versus amplitude of the magnetic anomaly at the surface for 13 wells. The systematic variation suggests that there is a physical relationship between the source of the magnetic anomaly and the source of the heat.

SUMMARY OF CHARACTERISTICS

Geology

(1) Sediments within the field can be characterized as a three-layer sequence of cap rock, slightly altered reservoir rock and more extensively altered reservoir rock. The sharp transition between the cap rock and the underlying reservoir rock is interpreted to represent the boundary between lacustrine sediments deposited in the isolated Salton Trough, and earlier marine sediments deposited in the Gulf of California.

(2) The cap rock is a variably thick, low permeability rock overlying the reservoir rock. In the upper 200 m, it consists of unconsolidated clay, silt, sand, and gravel. Below 200 m, it consists primarily of anhydrite-rich evaporite layers.

(3) The slightly altered reservoir rocks were subject to silicification and clay mineral reactions; however, these alterations did not change the petrophysical properties.

(4) Epidote and silica are the principal pore filling minerals produced during high temperature alteration. They replace calcite and anhydrite and a reduction of porosity and permeability within the altered reservoir zone results.

(5) Anhydrite veins reveal two or more episodes of fracturing and deposition indicating that the loss of permeability resulting from hydrothermal alteration is countered by the continuous development of new fractures.

(6) Correlations of data from well logs indicate that the sediments form a broad syncline with an east-west axis approximately perpendicular to the axis of the Salton Trough.

(7) Igneous activity in the Sea Geothermal Field is of 1–2 km within the field.

Geophysics

(1) The field is bounded by an intrusion of dike in the north of both (Biehler and Kelley, 1971).

(2) The field is bounded by the presence of igneous rocks (Kelley and Soske, 1971).

(3) The resistivity of the brine. The conductivity of the drilled field, based on the valley (Meidinger, 1971).

(4) Seismic refraction data within 1 km of the field.

(5) Numerous earthquakes (Schnapp and Fuijita, 1971).

(6) Interpretation of seismic locations, and gravity data (several steeply dipping faults, Frith, 1971; Meidinger, 1971; Frith, 1978).

Geothermal

(1) Equilibrium temperatures are extremely high (200°C higher than surface) within the valley.

(2) Within the field, temperature gradients near the surface are of depth of approximately 100 m.

(3) At the margin of the field, gradients at the surface are steep.

(4) Surface gradients of the field are approached as the surface is approached.

(5) The thermal gradient through the lithologic cap; it varies smoothly with the cap varies smoothly.

(6) Heat transfer through the cap, the upper thermal cap.

(7) Igneous activity is evidenced by five rhyolite buttes within the Salton Sea Geothermal Field. Basaltic and silicic dikes and sills are observed at depths of 1–2 km within the field (Robinson et al., 1976).

Geophysics

(1) The field is associated with a local gravity high, probably resulting from intrusion of dike material, or of hydrothermal alteration of the sediment, or of both (Biehler et al., 1964).

(2) The field is associated with a magnetic anomaly that probably reflects the presence of igneous material near the surface (Griscom and Muffler, 1971; Kelley and Soske, 1936).

(3) The resistivity anomaly probably reflects the boundary of the saline brine. The conductance of the sedimentary sequence is greatest in the area of the drilled field, but a broad area of high conductance extends along the axis of the valley (Meidav et al., 1976; Kasameyer, 1976).

(4) Seismic refraction data reveal the presence of high-velocity material within 1 km of the surface (Frith, 1978).

(5) Numerous earthquakes indicate that the area is tectonically active (Schnapp and Fuis, 1977).

(6) Interpretations of resistivity surveys, seismic refraction data, earthquake locations, and ground magnetic surveys are suggestive of the existence of several steeply dipping faults within the field (Muffler and White, 1968; Babcock, 1971; Meidav and Furgerson, 1972; Towse, 1975; Gilpin and Lee, 1978; Frith, 1978).

Geothermal

(1) Equilibrium temperature analysis indicates that the field is characterized by extremely high temperatures at depth. Temperatures at a depth of 2 km are 200°C higher than temperatures at similar depths in nongeothermal areas within the valley.

(2) Within the field, temperature profiles are characterized by high temperature gradients near the surface. There is a dramatic reduction in gradient at a depth of approximately 700 m.

(3) At the margin of the field, temperature profiles are characterized by low gradients at the surface and an increase in temperature gradient with depth.

(4) Surface gradients within the field are fairly constant, averaging 0.36°C/m. Surface gradients drop off rapidly to the regional value as the margin of the field is approached.

(5) The thermal cap does not necessarily conform in thickness to the lithologic cap; it varies irregularly. However, the temperature at the base of the cap varies smoothly with distance from the volcanic buttes.

(6) Heat transfer mechanisms can be modeled as a three-layer system. Layer 1, the upper thermal cap, is impermeable to fluid flow and has a high temper-

ature gradient consistent with conduction. Layer 2, still within the thermal cap but below the lithologic cap rock, has an increase in high-conductivity sand units that produce a lower temperature gradient. Layer 3, below the thermal cap, is characterized by low thermal gradients consistent with convective flow of pore fluid.

(7) A variety of evidence suggests that vertical convective motion within the reservoir is confined to small units. Vertical permeability is too low to allow for large-scale convection cells. Convection in the upper part of the reservoir is limited to individual sand bodies. Minor fractures in the lower reservoir allow for more extensive convective patterns. Major faults have not served as avenues of fluid and heat transport (Kendall, 1976).

(8) Superimposed on the small-scale convection could be a large-scale horizontal flow that transfers heat from the area of the buttes to the margins of the field.

A schematic section of the field, which relates the geological characteristics and the heat transfer characteristics, is seen in Fig. 20. Geologically, the section can be broken down into four layers (cap rock, slightly altered reservoir rock, highly altered reservoir rock, and zone of intrusion). The impermeable cap rock

Unit	Lithology	Heat transfer
Cap rock	Thick unconsolidated silt, sand, gravel, and anhydrite-rich deposits	Heat flow by conduction
Slightly altered reservoir	Shale and sand Small sand units	Enhanced conductivity resulting from presence of sand; still part of thermal cap
	Upper reservoir Shales, siltstone, and sandstone cemented by calcite or silica	Convection within sand units; shales separate region into isolated hydrologic systems
	Major shale break	
Highly altered reservoir	Lower reservoir Reduced permeability results when altered by replacement of calcite with epidote; extensively fractured	Fractures allow more extensive convection patterns
Zone of intrusion	Intrusion of small basaltic dikes and sills into sedimentary section; less than 20% intrusive bodies	Rate of heat release is a function of rate of intrusion

Fig. 20. The relationship between the lithology and the heat transfer characteristics at different zones from cap rock down to zone of intrusion.

is underlain by t
voir has undergc
properties. Basal
On the basis of t
layers. The then
cludes the cap ro
beds are thin. Th
voir. Small-scale
flow of pore flui
The rate of heat
a future paper w
evaluating a syst

ACKNOWLEDGEMENTS

We benefited
Larry Owen, Jac
Lila Abrahamson
getting the manu
of the Office of
of the Departme
This work wa
Energy by Lawr
W-7405-Eng-48.

REFERENCES

Babcock, E.A., 197
in the Imperial
Batze, M.L. and Si
Earth Plant. Sci.
Berner, R.A., 1971
241 pp.
Biehler, S., 1971. G
physical Investig
University of Ca
Biehler, S. and Lee
DLRI Rep. No.
Biehler, S., Kovach
of Gulf of Calif
Chan, M.A. and Te
Salton Sea Geot
Calif.
Combs, J. and Had
Anomaly, Impe
Dibblee, T.W., Jr.,
Jahns (Editor), (

still within the thermal
se in high-conductivity sand
yer 3, below the thermal
stent with convective flow

veective motion within the
bility is too low to allow
per part of the reservoir
in the lower reservoir
faults have not served as

ould be a large-scale
he buttes to the margins

geological characteristics
0. Geologically, the section
ly altered reservoir rock
The impermeable cap rock

Heat transfer
Heat flow by conduction

Enhanced conductivity
resulting from presence
of sand; still part of thermal
cap

Convection within sand
units; shales separate region
into isolated hydrologic
systems

Fractures allow more
intensive convection
patterns

Rate of heat release
function of rate
of intrusion

Transfer characteristics at

is underlain by the dominantly sand reservoir. The lower portion of the reservoir has undergone hydrothermal alteration, which changed the petrophysical properties. Basaltic and silicic dikes penetrate to within 1 km of the surface. On the basis of thermal properties, the field can be broken down into three layers. The thermal cap is characterized by conductive heat transfer and includes the cap rock and an upper portion of the sand reservoir where the sand beds are thin. The convective zone includes the major portion of the sand reservoir. Small-scale cellular convection is superimposed upon a large-scale lateral flow of pore fluid. The heat source region corresponds to the zone of intrusion. The rate of heat release in this region is a function of the rate of intrusion. In a future paper we will use these observations as a basis for establishing and evaluating a system model.

ACKNOWLEDGEMENTS

We benefited from discussions with numerous colleagues, most notably Larry Owen, Jack Howard, Jon Hanson, and Don Towse. The assistance of Lila Abrahamson, of the Technical Information Department at LLNL, in getting the manuscript into final form is appreciated. We acknowledge support of the Office of Basic Energy Sciences and the Division of Geothermal Energy of the Department of Energy.

This work was performed under the auspices of the U.S. Department of Energy by Lawrence Livermore National Laboratory under contract No. W-7405-Eng-48.

REFERENCES

- Babcock, E.A., 1971. Detection of active faulting using oblique infrared aerial photography in the Imperial Valley of California. *Geol. Soc. Am. Bull.*, 82: 3189-3196.
- Batzle, M.L. and Simmons, G., 1976. Microfractures in rocks from two geothermal areas. *Earth Plant. Sci. Lett.*, 30: 71-93.
- Berner, R.A., 1971. *Principles of Chemical Sedimentology*. McGraw-Hill, New York, N.Y., 241 pp.
- Biehler, S., 1971. Gravity studies in the Imperial Valley. In: *Cooperative Geological-Geophysical Investigations of Geothermal Resources in the Imperial Valley Area of California*. University of California, Riverside, Calif., pp. 29-41.
- Biehler, S. and Lee, T., 1977. Final report on a resource assessment of the Imperial Valley. DLRI Rep. No. 10, Univ. Calif., Riverside, Calif., 61 pp.
- Biehler, S., Kovach, R.L. and Allen, C.R., 1964. Geophysical framework of northern end of Gulf of California Structural Province. *Am. Assoc. Pet. Geol., Mem.*, 3: 126-143.
- Chan, M.A. and Tewhey, J.D., 1977. Subsurface structure of the southern portion of the Salton Sea Geothermal Field. UCRL-523554, Lawrence Livermore Natl. Lab., Livermore, Calif.
- Combs, J. and Hadley, D., 1977. Microearthquake investigation of the Mesa Geothermal Anomaly, Imperial Valley, California. *Geophysics*, 42: 17-33.
- Dibblee, T.W., Jr., 1954. Geology of the Imperial Valley Region, California, Pt. 2. In: R.H. Jahns (Editor), *Geology of Southern California*. Calif. Div. Mines Bull., 170: 21-28.

- Downs, T. and Woodward, G.D., 1961. Middle Pleistocene extension of the Gulf of California into the Imperial Valley. *Geol. Soc. Am. Abstr. Spec. Paper*, 68: 21.
- Dutcher, L.C., Hardt, W.F. and Moyle, W.R., Jr., 1972. Preliminary appraisal of ground water in storage with reference to geothermal resources in the Imperial Valley Area, California. *U.S. Geol. Surv., Circ.*, 649.
- Elder, J.W., 1967. Steady free convection in a porous medium heated from below. *J. Fluid Mech.*, 27: 29-48.
- Elders, W.A. and Biehler, S., 1975. Gulf of California rift system and its implication for the tectonics of western North America. *Geology* 3(2): 85-87.
- Elders, W.A., Rex, R.W., Meidav, T., Robinson, P.T. and Biehler, S., 1972. Crustal spreading in Southern California. *Science*, 178: 15-24.
- Facca, G., 1973. The structure and behavior of geothermal fields. In: H.C.H. Armstead (Editor), *Geothermal Energy, Review of Research and Development*. United Nations Educational, Scientific and Cultural Organization, Paris, pp. 61-69.
- Facca, G. and Tonani, F., 1967. The self-sealing geothermal field. *Bull. Volcanol.*, 30: 271-273.
- Frith, R.B., 1978. A seismic refraction investigation of the Salton Sea Geothermal area, Imperial Valley California. M.S. Thesis, University of California, Riverside, Calif., 94 pp. (unpublished).
- Fuis, G.S., Mooney, W.D., Healey, J.H., McMechan, G.A. and Lutter, W.J., 1982. Crustal structure of the Imperial Valley. *U.S. Geol. Surv., Prof. Pap.* 1254, in press.
- Gilpin, B. and Lee, Tien-Chang, 1978. A microearthquake study in the Salton Sea Geothermal area, California. *Bull. Seismol. Soc. Am.*, 68: 441-450.
- Grindley, G.W. and Browne, P.R.L., 1976. Structural and hydrological factors controlling the permeabilities of some hot-water geothermal wells. In: *Proceedings Second United Nations Symposium on Development and Use of Geothermal Resources, Vol. 1*. Lawrence Berkeley Laboratory, Berkeley, Calif., pp. 379-386.
- Griscom, A. and Muffler, L.J.P., 1971. Aeromagnetic map and interpretation of the Salton Sea geothermal area, California. *U.S. Geol. Surv., Geophys. Invest. Map*, GP 754.
- Hamilton, W., 1961. Origin of the Gulf of California. *Geol. Soc. Am. Bull.*, 72: 1307-1318.
- Helgeson, H.C., 1968. Geologic and thermodynamic characteristics of the Salton Sea geothermal system. *Am. J. Sci.*, 266(3): 129-166.
- Hill, D.P., 1977. A model for earthquake swarms, *J. Geophys. Res.*, 82: 1347-1352.
- Hill, D.P., Mowinkel, P. and Peake, L.G., 1975. Earthquake active faults and geothermal areas in the Imperial Valley, California. *Science*, 188: 1306-1308.
- Johnson, C.E., 1979. I: CEDAR - an approach to the computer automation of short-period local seismic networks. II: Seismotectonics of the Imperial Valley of Southern California. Ph.D. Dissertation, California Institute of Technology, Pasadena, Calif.
- Kasameyer, P.W., 1976. Preliminary interpretation of resistivity and seismic refraction data from the Salton Sea Geothermal Field. UCRL-52115. Lawrence Livermore Natl. Lab., Livermore, Calif.
- Keller, G.V. and Frischknecht, F.C., 1966. *Electrical Methods in Geophysical Prospecting*. Pergamon Press, New York, N.Y., 517 pp.
- Kelley, V.C. and Soske, J.L., 1936. Origin of the Salton volcanic domes, Salton Sea, California. *J. Geol.*, 44: 496-509.
- Kendall, C., 1976. Petrology and stable isotope geochemistry of three wells in the Buttes area of the Salton Sea Geothermal Field, Imperial Valley California, U.S.A. M.S. Thesis, University of California, Riverside, Calif. (unpublished).
- Lee, T. and Cohen, L., 1977. Onshore and offshore measurements of temperature gradients in the Salton Sea geothermal area, California. UCR/I6PP-77/22, Univ. Calif., Riverside, Calif.
- Lofgren, B.E., 1978. Salton Trough continues to deepen in Imperial Valley, California. *Trans. Am. Geophys. Union*, 59: 1051.
- Lomnitz, C., Mooser
Gulf of California
McDowell, S.D. and
thermal Field, Ca
and temperature
McDowell, S.D. and
Salton Sea Geoth
Calif., Riverside,
Meidav, T. and Furg
area, California. (C
Meidav, T., West, R.
of the Salton Sea
Livermore Natl.)
Morse, J.G. and The
Sea Geothermal i
Muffler, L.J.P. and
Southeastern Cal
Prague; 97 (Sym)
Muffler, L.J.P. and
in the Salton Sea
Geol. Soc. Am. I
Nathenson, M. and
systems and con
the United State
Palmer, T.D., 1975.
Field, Imperial C
more, Calif.
Randall, W., 1974.
Sea geothermal f
ornia, Riverside
Renner, J.L., White
Assessment of G
Robinson, P.T., Eld
Salton Sea Geotl
360.
Schnapp, M. and Fu
Imperial Valley,
mological Labor
Skinner, B.J., White
Salton Sea Geotl
Storre, B. and Nitsc
cite + 1 H₂O. Co
Sylvester, A.G., 19
reported by T.A
Tewhey, J.D., 1977
Field. UCRL-52
Towse, D., 1975. A
California. UCR
Towse, D.F. and P
geothermal test
Van de Kamp, P.C.
California: a rec

- sion of the Gulf of
ec. Paper, 68: 21.
ary appraisal of ground
Imperial Valley Area,
eated from below. *J. Fluid*
and its implication for
7.
S., 1972. Crustal spread
s. In: H.C.H. Armstead
pment. United Nations
1-69.
l. *Bull. Volcanol.*, 30: 271-
n Sea Geothermal area,
ia, Riverside, Calif., 94
tter, W.J., 1982. Crustal
254, in press.
in the Salton Sea Geo-
0.
ogical factors controlling
ceedings Second United
Resources, Vol. 1.
6.
terpretation of the
ys. Invest. Map, GP 754
Am. Bull., 72: 1307-1318
cs of the Salton Sea
s., 82: 1347-1352.
e faults and geothermal
308.
utomation of short-
rial Valley of Southern
y, Pasadena, Calif.
d seismic refraction
rence Livermore Natl.
Geophysical Prospecting
omes, Salton Sea,
ree wells in the Buttes
rnia, U.S.A. M.S. Thesis
of temperature gradients
Univ. Calif., Riverside,
l Valley, California.
- Lomnitz, C., Mooser, F., Allen, C., Brune, J.N. and Thatcher, W., 1970. Seismicity of the Gulf of California region, Mexico — preliminary results. *Geofis. Int.*, 10: 37-48.
- McDowell, S.D. and McCurrey, M., 1977. Active metamorphism in the Salton Sea Geothermal Field, California: mineralogical and mineral chemistry changes with depth and temperature in sandstone. *Geol. Soc. Am. Abstr. Prog.*, 9(7): 1088.
- McDowell, S.D. and Elders, W.A., 1979. Geothermal metamorphism of sandstone in the Salton Sea Geothermal System. UCR/I6PP-79-25, Inst. Geophys. Planet. Phys., Univ. Calif., Riverside, Calif.
- Meidav, T. and Furgerson, R., 1972. Resistivity studies of the Imperial Valley geothermal area, California. *Geothermics*, 1: 47-62.
- Meidav, T., West, R., Katzenstein, A. and Rostein, Y., 1976. An electrical resistivity survey of the Salton Sea Geothermal Field, Imperial Valley California. UCRL-13690, Lawrence Livermore Natl. Lab. Livermore, Calif.
- Morse, J.G. and Thorson, L.D., 1978. Reservoir engineering study of a portion of the Salton Sea Geothermal Field. *Geotherm. Resour. Coun. Trans.*, 2: 471-474.
- Muffler, L.J.P. and White, D.E., 1968. Origin of CO₂ in the Salton Sea geothermal system, Southeastern California, U.S.A. In: *Proceedings 23rd International Geological Congress, Prague*, 97 (Symposium 2): 185-194.
- Muffler, L.J.P. and White, D.E., 1969. Active metamorphism of upper Cenozoic sediments in the Salton Sea Geothermal Field and the Salton Trough, Southeastern California. *Geol. Soc. Am. Bull.*, 80: 157-182.
- Nathenson, M. and Muffler, L.J.P., 1975. Geothermal resources in hydrothermal convection systems and conduction dominated areas. In: *Assessment of Geothermal Resources of the United States*. U.S. Geol. Surv., Circ., 726.
- Palmer, T.D., 1975. Characteristics of geothermal wells located in the Salton Sea Geothermal Field, Imperial County, California. UCRL-51976, Lawrence Livermore Natl. Lab., Livermore, Calif.
- Randall, W., 1974. An analysis of the subsurface structure and stratigraphy of the Salton Sea geothermal anomaly, Imperial Valley, California. Ph.D. Thesis, University of California, Riverside, Calif. (unpublished).
- Renner, J.L., White, D.E. and Williams, D.L., 1975. Hydrothermal convection systems. In: *Assessment of Geothermal Resources of the United States*. U.S. Geol. Surv., Circ., 726.
- Robinson, P.T., Elders, W.A. and Muffler, L.J.P., 1976. Quaternary Volcanism in the Salton Sea Geothermal Field, Imperial Valley, California. *Geol. Soc. Am. Bull.*, 87: 347-360.
- Schnapp, M. and Fuis, G., 1977. Preliminary Catalog of Earthquakes in the Northern Imperial Valley, October 1, 1976 to December 31, 1976. U.S. Geological Survey Seismological Laboratory, Pasadena, Calif.
- Skinner, B.J., White, D.E., Rose, H.J. and Mays, R.E., 1967. Sulfides associated with the Salton Sea Geothermal brine. *Econ. Geol.*, 62(3): 316-330.
- Storre, B. and Nitsch, K.H., 1972. Die Reaktion $2 \text{Zoisite} + 1 \text{CO}_2 \rightleftharpoons 3 \text{Anorthite} + 1 \text{Calcite} + 1 \text{H}_2\text{O}$. *Contrib. Mineral. Petrol.*, 35: 1-10.
- Sylvester, A.G., 1979. Earthquake damage in Imperial Valley, California, May 18, 1940, as reported by T.A. Clark. *Bull. Am. Seismol. Soc.*, 69: 547-568.
- Tewhey, J.D., 1977. Geologic characteristics of a portion of the Salton Sea Geothermal Field. UCRL-52267, Lawrence Livermore Natl. Lab., Livermore, Calif.
- Towse, D., 1975. An estimate of the geothermal energy resource in the Salton Trough California. UCRL-51851, Lawrence Livermore Natl. Lab., Livermore, Calif.
- Towse, D.F. and Palmer, T.D., 1975. Summary of geology at the ERDA-Magma-SDG&E geothermal test site. UCID-17008, Lawrence Livermore Natl. Lab., Livermore, Calif.
- Van de Kamp, P.C., 1973. Holocene continental sedimentation in the Salton Basin, California: a reconnaissance. *Geol. Soc. Am. Bull.*, 84: 827-848.

- Weaver, C.S. and Hill, D.P., 1978. Earthquake swarms and local crustal spreading along major strike-slip faults in California. *Pure Appl. Geophys.*, 177: 51-64.
- White, D.E., 1968. Environments of generation of some base metal ore deposits. *Econ. Geol.*, 63(4): 301-335.
- Yunker, L. and Kasameyer, P.W., 1978. A revised estimate of recoverable thermal energy in the Salton Sea Geothermal resource area. UCRL-52450, Lawrence Livermore Natl. Lab., Livermore, Calif.

GEOCHEMISTRY
VOLCANIC ROCKS

PAUL K. HÖRMANN
Mineralogisch-Petro-
Kiel (Federal Republ
Mineralogisch-Petro-
Tübingen (Federal I
(Received March 10

ABSTRACT

Hörmann, P.K. and
volcanic rocks of
259-282.

The Cenozoic volcanic rocks of the western Cordillera (Western Cordillera) series which is characterized by high abundances of large ion incompatible elements (Zr, U, Th). The magmas of the dacite-rhyolite series have higher Cr versus MgO correlation coefficients than in the rocks of the Sub-Andean series. The rocks are chemically similar to the Basic Igneous Compositions of the Andes.

It is suggested that the Cordillera originated from the BIC-type in a tectonic setting which corresponds to the

INTRODUCTION

The Andes of South America, are a famous volcanic belt, are a famous volcanic belt at the margins. Miyashiro (1977) and calc-alkaline